RSC Advances

PAPER

View Article Online
View Journal | View Issue

Cite this: *RSC Adv.*, 2021, **11**, 11062

A network pharmacology study on main chemical compounds from *Hibiscus cannabinus* L. leaves†

Ki Kwang Oh,[a] Md. Adnan,[a] Inseok Ju[b] and Dong Ha Cho*[a]

Hibiscus cannabinus L. leaves (HCLLs) are considered a favorable source of natural antiobesity substances. However, actual bioactive compound(s) in it and their mechanism(s) against obesity have not been confirmed. Hence, network pharmacology was conducted to identify its key compounds and mechanism(s) against obesity. Compounds in HCLLs were identified through GC-MS analysis and screened by Lipinski's rule. Genes related to the selected compounds and obesity were obtained from public databases, and overlapping genes between HCLL compound-related genes and obesity target genes were selected using a Venn diagram. The networking between selected compounds and overlapping genes was then constructed, visualized, and analyzed by RStudio. Finally, the binding affinity between compounds and genes was evaluated *via* molecular docking (MD). A total of 30 compounds in HCLLs were detected *via* GC-MS, and Lipinski's rule accepted all compounds. The compound-related genes (570 genes) and obesity targeted genes (3028 genes) were identified, and between them, 64 overlapping genes were selected. Gene Set Enrichment Analysis (GSEA) displayed that the mechanisms of HCLLs against obesity were associated with 13 signaling pathways on 22 compounds in HCLLs. Superficially, AKT1, vitamin E, and RAS signaling pathways were noted as a hub gene, an uppermost bioactive compound, and a hub signaling pathway, respectively. However, the binding affinity of ligands and proteins on the RAS signaling pathway was very low; instead, the PPAR signalling pathway was evaluated with potent efficacy against obesity through MD. On the PPAR signaling pathway, α-amyrin was found as the most significant compound for the amelioration of obesity. α-Amyrin manifested the strongest binding affinity on six target proteins associated with the PPAR signaling pathway. Our study suggests that an auxiliary (PPAR) signaling pathway of HCLLs might intervene efficiently against obesity over the hub (RAS) signaling pathway.

Received 30th December 2020
Accepted 3rd March 2021

DOI: 10.1039/d0ra10932k

rsc.li/rsc-advances

1. Introduction

Obesity is a perplexing health issue, it can cause diabetes, heart failure, stroke, and some types of cancer, and is linked to deaths worldwide.[1] Obesity is characterized by excessive body fat, wherein the body mass index (BMI) reaching more than thirty is considered obesity.[2] Obesity can appear at any age; about 13% (11% of men and 15% of women) of adults and 7% (6% of girls and 8% of boys) of children and adolescents were obese in 2016.[3] Obesity also gives to rise an enormous burden on individual, family members, and even nations, resulting in economic disadvantages.[4] The main driving factor of obesity is the breaking down oily compounds (from food sources) into small glycerol molecules and fatty acids that are absorbed quickly in human cells and accumulate in the body. In this regard, the inhibition of metabolism can be a critical therapeutic strategy.[5] Currently, antiobesity drugs are being used to inhibit intestinal fat absorption (Orlistat). Also, suppressing appetite (diethylpropion, fenfluramine, sibutramine, rimonabant) is another strategy followed by most countries to control obesity.[6] However, recent researches revealed that herbal plants might play a significant role in treating obesity, and among various plants, Kenaf (*Hibiscus cannabinus* L.) leaves are reported to be effective for antiobesity.[7,8] Moreover, our previous studies proved that various kenaf parts have promising biological activities.[9–12] To date, natural plant products are used as dietary supplements and further therapeutic agents for health promotion to prevent obesity.[13]

A study showed that administration of *H. cannabinus* extract to female Wistar albino rats fed with a high cholesterol diet significantly reduced the level of serum cholesterol, triglycerides, and low-density lipoprotein cholesterol (LDL-C).[14] In addition, obesity-induced heart failure and hypertension can be ameliorated by the presence of abundant polyphenols and

[a]*Department of Bio-Health Convergence, College of Biomedical Science, Kangwon National University, Chuncheon, 24341, Korea. E-mail: chodh@kangwon.ac.kr; nivirna07@kangwon.ac.kr; mdadnan1991.pharma@gmail.com; Tel: +82-33-250-6475*

[b]*Department of Bio-Health Technology, College of Biomedical Science, Kangwon National University, Chuncheon, 24341, Korea. E-mail: sherpa7@kangwon.ac.kr*

† Electronic supplementary information (ESI) available. See DOI: 10.1039/d0ra10932k

flavonoids in HCLLs.[15] At present, uppermost bioactive compounds and mechanisms of HCLLs against obesity have remained unknown, and should be strengthened to foster pharmacological evidence to provide its therapeutic application in ameliorating obesity.

By utilizing a suitable analytical method, "network pharmacology", it is possible to systematically evaluate the complex compound-gene and compound–therapeutics interactions, thus, determining a prototype for efficient treatment.[16,17] Network pharmacology can be used to discover novel mechanisms of drugs, holistically, which is directed to a paradigm instead of "multiple targets, multiple diseases" of "one target, one disease".[18] Therefore, it is an efficient approach to select potential lead compounds (from natural sources) with a specific mechanism of action for the amelioration of various diseases, and mostly to elucidate the synergistic efficacy of bioactive compounds.[19]

A report indicated that progressive development of bioinformatics, systems biology, and poly-pharmacology facilitates a network-based drug discovery, which is considered as an efficient new drug development method.[20] Another report explicated that network pharmacology is utilized as a powerful tool to understand the pharmacological mechanism(s) between the traditional Ge-Gen-Qin-Lian Decoction (GGQLD) formula and target genes.[21] Furthermore, the development of bioinformatics contributes significantly to the methodology of network pharmacology. For instance, Dr Shoichet's group developed the 'Similarity Ensemble Approach' (SEA) to search the ligand–target interaction and ultimately understand its association.[22] Also, SwissTargetPrediction (STP) is an online tool developed by SIB (Swiss Institute of Bioinformatics), which uploaded 376 342 experimentally approved molecules and 3068 protein targets since 2014.[23] In this work, we utilized the two-bioinformatics tools to construct the ligand–protein interaction. To sum things up, network pharmacology *via* the bioinformatics tool was utilized to investigate the chemical constituents and mechanism(s) of HCLLs against obesity. The analysis processing is shown in Fig. 1.

2. Materials and methods

2.1 Plant material collection and identification

Hibiscus cannabinus L. leaves (HCLLs) were collected from Pyeonghwa-ro of Chuncheon-si (latitude: 37.885596, longitude: 127.730032), Gangwon-do, Republic of Korea, in September 2020, and the plant was identified by Dr Dong Ha Cho, Plant biologist and Professor, Department of Bio-Health Convergence, College of Biomedical Science, Kangwon National University. A voucher number (KEN 305) has been deposited at Kenaf Corporation in the Department of Bio-Health Convergence, and the material can be only used for research.

2.2 Plant preparation, extraction

The collected HCLLs were dried at a shady area at room temperature (20–22 °C), and dried leaves were powdered using an electric blender. Approximately 200 g of HCLLs powder was soaked in 500 mL of 100% methanol (Daejung, Korea) for 3 days and repeated 3 times to collect the extraction. The solvent extract was collected, filtered, and evaporated using a vacuum

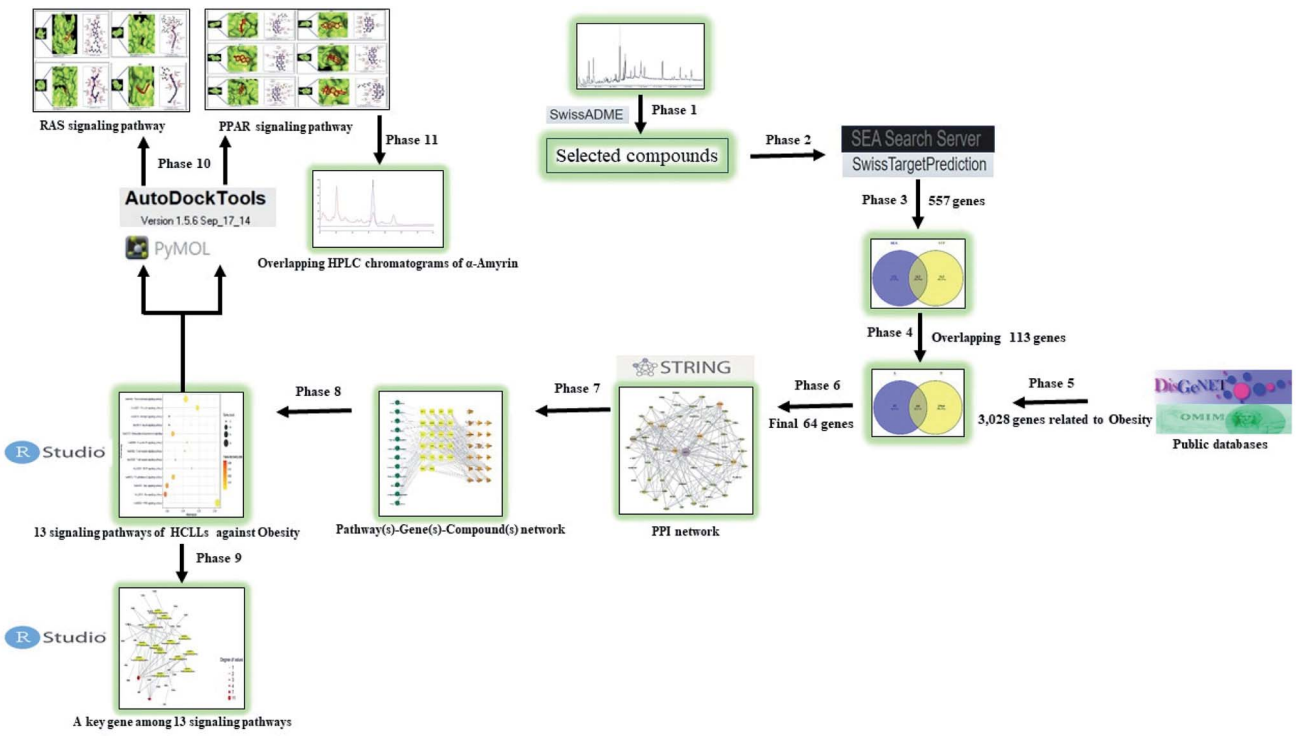

Fig. 1 Analytical processing steps of HCLLs against obesity.

evaporator (IKA-RV8, Japan). The evaporated sample was dried under a boiling water bath (IKA-HB10, Japan) at 40 °C to obtain the yield.

2.3 GC-MS analysis condition

Agilent 7890A was used to perform GC-MS analysis. The GC was equipped with a DB-5 (30 m × 0.25 mm × 0.25 μm) capillary column. Initially, the instrument was maintained at a temperature of 100 °C for 2.1 minutes. The temperature rose to 300 °C at a rate of 25°C min^{-1} and was maintained for 20 minutes. Injection port temperature and helium flow rate were ensured as 250 °C and 1.5 mL min^{-1}, respectively. The ionization voltage was 70 eV. The samples were injected in a split mode at 10 : 1. The MS scan range was set at 35–900 (m/z). The fragmentation patterns of mass spectra were compared with those stored in the W8N05ST library MS database. The percentage of each compound was calculated from the relative peak area of each compound in the chromatogram. The concept of integration was used the ChemStation integrater algorithms.[24]

2.4 Chemical compounds database construction and drug-likeness filtering

The information about chemical compounds from HCLLs was identified through GC-MS analysis. GC-MS detected 30 compounds filtered according to Lipinski's rule through SwissADME (http://www.swissadme.ch/) to identify the "Drug-likeness" property. The PubChem (https://pubchem.ncbi.nlm.nih.gov/) was utilized to identify the SMILES (Simplified Molecular Input Line Entry System) of compounds.

2.5 Target genes related to selected compounds or obesity

Based on the SMILES, target genes linked to the compounds were selected through both Similarity Ensemble Approach (SEA) (http://sea.bkslab.org/) and SwissTargetPrediction (STP) (http://www.swisstargetprediction.ch/) with "*Homo Sapiens*" setting. Obesityrelated genes were identified by DisGeNET (https://www.disgenet.org/search) and OMIM (https://www.ncbi.nlm.nih.gov/omim) databases. The overlapping genes between compounds of HCLLs and obesity target genes were identified and visualized by VENNY 2.1 (https://bioinfogp.cnb.csic.es/tools/venny/).

2.6 Network construction of interacted overlapping genes

The final overlapping genes input in the STRING database with *Homo sapience* mode identified signaling pathways connected to the final overlapping genes. A bubble chart analyzed the identified signaling pathways through RStudio. The bubble chart shows a hub signaling pathway (the lowest rich factor) and an auxiliary signaling pathway (the highest rich factor) between bioactive compounds and obesity targeted genes of HCLLs.

2.7 Preparation for MD of target proteins

Four target proteins of a hub signaling pathway *i.e.*, AKT1 (PDB ID: 1UNQ), PRKCA (PDB ID: 3IW4), PLA2G4A (PDB ID: 1KVO), and PLA2G2A (PDB ID: IBCI) were selected on STRING *via* RCSB PDB (https://www.rcsb.org/). Six target proteins of an auxiliary signaling pathway, *i.e.*, NR1H3 (PDB ID: 2ACL), PPARA (PDB ID: 3SP6), PPARD (PDB ID: 5U3Q), PPARG (PDB ID: 3E00), FABP3 (PDB ID: 5HZ9), and FABP4 (PDB ID: 3P6D) were selected on STRING *via* RCSB PDB (https://www.rcsb.org/). The proteins selected in the .pdb format were converted into the .pdbqt format *via* Autodock (http://autodock.scripps.edu/).

2.8 Preparation for MD of positive control compounds

Five positive control compounds on PPARA agonists, *i.e.*, clofibrate (PubChem ID: 2196), gemfibrozil (PubChem ID: 3463), cprofibrate (PubChem ID: 2763), bezafibrate (PubChem ID: 39042), fenofibrate (PubChem ID: 3339) were selected to identify the docking score. One positive control compound on PPARD agonist, *i.e.*, cardarine (PubChem ID: 9803963), was selected to identify the docking score. Three positive control compounds on PPARG agonists, *i.e.*, pioglitazone (PubChem ID: 4829), Rosiglitazone (PubChem ID: 77999), Lobeglitazone (PubChem ID: 9826451), were selected to identify the docking score.

2.9 Preparation for MD of ligand molecules

The ligand molecules were converted from .sdf from PubChem into .pdb format using Pymol, and the ligand molecules were converted into .pdbqt format through Autodock.

2.10 Ligand–protein docking

The ligand molecules were docked with target proteins utilizing autodock4 by setting-up 4 energy ranges and 8 exhaustiveness as default to obtain 10 different poses of ligand molecules.[25] The active site's grid box size was $x = 20.973$ Å, $y = 25.96$ Å and $z = 41.239$ Å. The 2D-binding interactions were identified through LigPlot+ v.2.2 (https://www.ebi.ac.uk/thornton-srv/software/LigPlus/). After docking, ligands of the lowest binding energy (highest affinity) were selected to visualize the ligand–protein interaction in pymol.

2.11 Chemicals and reagents for HPLC analysis

Standard α-amyrin was purchased from Sigma Aldrich (USA). HPLC grade acetonitrile was obtained from Burdick & Jackson. Ultrapure water obtained using a Milli-Q UF-Plus instrumentation (Millipore, MA, USA) was utilized to prepare all solutions for the method.

2.12 Instrumentation and chromatographic conditions

HPLC Agilent 1260 series chromatographic instrumentation was used in this research. Data were collected and processed with the Agilent 1260 chemstation. The HPLC system was equipped with an injection valve, quaternary gradient pump

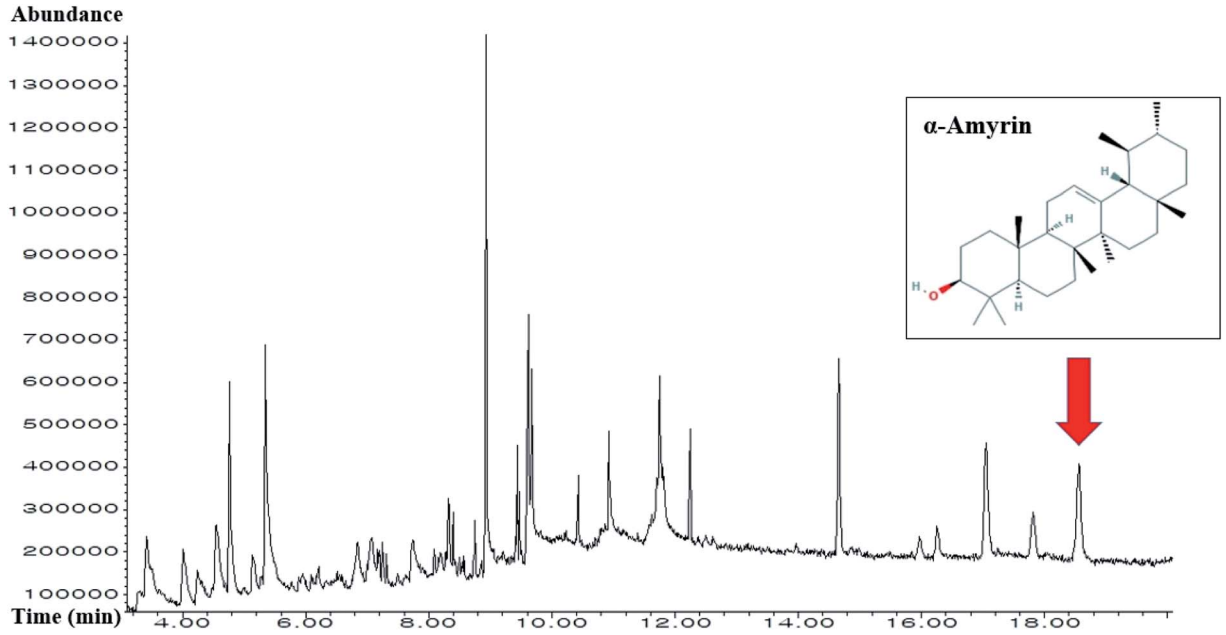

Fig. 2 GC-MS chromatogram of methanolic extract of HCLLs and indication of α-amyrin.

system, and UV dual λ absorbance detector. Chromatographic separation was performed on a C18 column 4.6 × 150 mm, 3.5 μm. The mobile phase was isocratic acetonitrile 95% (95 : 5, v/v, acetonitrile : water) at a flow rate of 10 μL min^{-1}. Its analysis was performed at ambient temperature, and detection was made at 200 nm. The injected volume was 20 μL.

Table 1 A list of the identified 30 chemical compounds from HCLLs through GC-MS

No.	Compounds	PubChem ID	RT (mins)	Area (%)
1	1-Methoxycyclohexa-1,3-diene	75098	3.414	5.23
2	1-Methyl-3-piperidinol	98016	4.01	2.74
3	2,4-Diamino-6-pyrimidinone	135408763	4.241	1.79
4	3,4-Pentadienal	534089	4.549	4.19
5	3-Hydroxy-2,3-dihydromaltol	119838	4.77	4.99
6	5-(Hydroxymethyl)furfural	237332	5.347	9.54
7	1-Octanamine	8143	6.847	2.58
8	Propanoic acid, 3-hydroxy-	68152	7.077	2.83
9	2-Thio-6-azauracil	1275976	7.174	0.58
10	4-Ethyl-2,5-dimethylisoxazolidine, (*E*)-	22212544	7.202	0.52
11	2,5-Dimethoxy-4-methylbenzaldehyde	602019	7.25	0.78
12	*N*-Hydroxymethylacetamide	69365	7.318	0.32
13	2-Furanone	140765	7.741	2.57
14	2,3-Dihydro-5*H*-1,4-dioxepine	536111	8.202	1.35
15	Oleic acid	445639	8.279	0.54
16	Loliolide	100332	8.327	1.77
17	Citronellylacetone	102604	8.395	1.23
18	Cyclopentaneundecanoic acid, methyl ester	535041	8.75	0.88
19	Palimitic acid	985	9.039	0.85
20	Methyl elaidolinolenate	5367462	9.443	1.65
21	Phytol	5366244	9.481	0.93
22	Linolenyl alcohol	6436081	9.616	4.26
23	Stearic acid	5281	9.674	3.31
24	Octyl adipate	7641	10.424	0.78
25	Monopalmitin	14900	10.933	3.66
26	9,12,15-Octadecatrienol	68169	11.75	7.31
27	Squalene	638072	12.25	1.72
28	Vitamin E	14985	14.664	5.19
29	Clionasterol	457801	17.058	4.70
30	α-Amyrin	73170	18.558	4.59

2.13 Preparation of standard solution

A stock solution of standard (α-amyrin) was prepared in MeOH. The prepared stock solutions of concentrations 7.8125, 16.625, 31.25, 62.5, 125, and 250 ppm were made to plot the standard curve.

2.14 Preparation of plant extraction for HPLC analysis

The 800 mg of HCLLs MeOH extraction was taken in a flask, 40 mL of MeOH was added and kept for 3 hours. After shaking several times, the extraction was left for 2 days at room temperature. The solution from the flask was filtered through a Whatman No. 1 filter paper. The filtered solution was passed through a 0.2 μm syringe filter and HPLC analysis was performed.

3. Results and discussion

3.1 Composition of potentially bioactive compounds from HCLLs

A total of 30 compounds in HCLLs were detected using the GC-MS analysis (Fig. 2), and the name of compounds, PubChem ID, retention time, peak area (%) are enlisted in Table 1. All 30 compounds were checked and accepted by Lipinski's rule (molecular weight ≤500 g mol^{-1}; moriguchi octanol–water partition coefficient ≤4.15; the number of nitrogen or oxygen ≤10; the number of NH or OH ≤5), and all compounds passed the standard of "Abbott Bioavailability Score (>0.1)" verified through SwissADME (Table 2).

3.2 Overlapping genes between SEA and STP networked with 30 compounds

Based on the SMILES, a total of 244 genes from SEA and 442 genes from STP connected to 30 compounds were extracted (ESI Table S1†). A Venn diagram showed that 116 genes were overlapped between the two public databases (Fig. 3).

3.3 Overlapping genes between obesity related genes and 116 overlapping genes

A total of 3028 genes related to T2DM were sorted by browsing DisGeNET and OMIM databases (ESI Table S2†). Venn

Table 2 Physicochemical properties of the 20 compounds for good oral bioavailability[a]

		Lipinski's rules					
		MW	HBA	HBD	Mlog *P*	Lipinski's violations	Bioavailability score
No.	Compounds	<500	<10	≤5	≤4.15	≤1	>0.1
1	1-Methoxycyclohexa-1,3-diene	110.15	1	0	1.24	0	0.55
2	1-Methyl-3-piperidinol	115.17	2	1	0.21	0	0.55
3	2,4-Diamino-6-pyrimidinone	126.12	2	3	−1.82	0	0.55
4	3,4-Pentadienal	82.10	2	1	0.81	0	0.55
5	3-Hydroxy-2,3-dihydromaltol	144.13	4	2	−1.77	0	0.85
6	5-(Hydroxymethyl)furfural	126.11	3	1	−1.06	0	0.55
7	1-Octanamine	129.24	1	1	2.22	0	0.55
8	Propanoic acid, 3-hydroxy-	90.08	3	2	−0.85	0	0.85
9	2-Thio-6-azauracil	129.14	2	2	−1.25	0	0.55
10	4-Ethyl-2,5-dimethylisoxazolidine, (*E*)-	129.20	2	0	1.38	0	0.55
11	2,5-Dimethoxy-4-methylbenzaldehyde	180.20	3	0	1.13	0	0.55
12	*N*-Hydroxymethylacetamide	89.09	2	2	−0.85	0	0.55
13	2-Furanone	84.07	2	0	−0.01	0	0.55
14	2,3-Dihydro-5*H*-1,4-dioxepine	100.01	2	0	−0.31	0	0.55
15	Oleic acid	282.46	2	1	4.57	1	0.85
16	Loliolide	196.24	3	1	1.49	0	0.55
17	Citronellylacetone	196.33	1	0	3.43	0	0.55
18	Cyclopentaneundecanoic acid, methyl ester	268.43	2	0	4.04	0	0.55
19	Palmitic acid	256.42	2	1	4.19	1	0.85
20	Methyl elaidolinolenate	292.46	2	0	4.61	1	0.55
21	Phytol	296.53	1	1	5.25	1	0.55
22	Linolenyl alcohol	264.45	1	1	4.59	1	0.55
23	Stearic acid	284.48	2	1	4.67	1	0.85
24	Octyl adipate	370.57	4	0	4.55	1	0.55
25	Monopalmitin	330.50	4	2	3.18	0	0.55
26	9,12,15-Octadecatrienol	264.45	1	1	4.59	1	0.55
27	Squalene	410.72	0	0	7.93	1	0.55
28	Vitamin E	430.71	2	1	6.14	1	0.55
29	Clionasterol	414.71	1	1	6.73	1	0.55
30	α-Amyrin	426.72	1	1	6.92	1	0.55

[a] MW, molecular weight (g mol^{-1}); HBA, hydrogen bond acceptor; HBD, hydrogen bond donor; log *P*, lipophilicity; bioavailability score, the ability of a drug or other substance to be absorbed and used by the body.

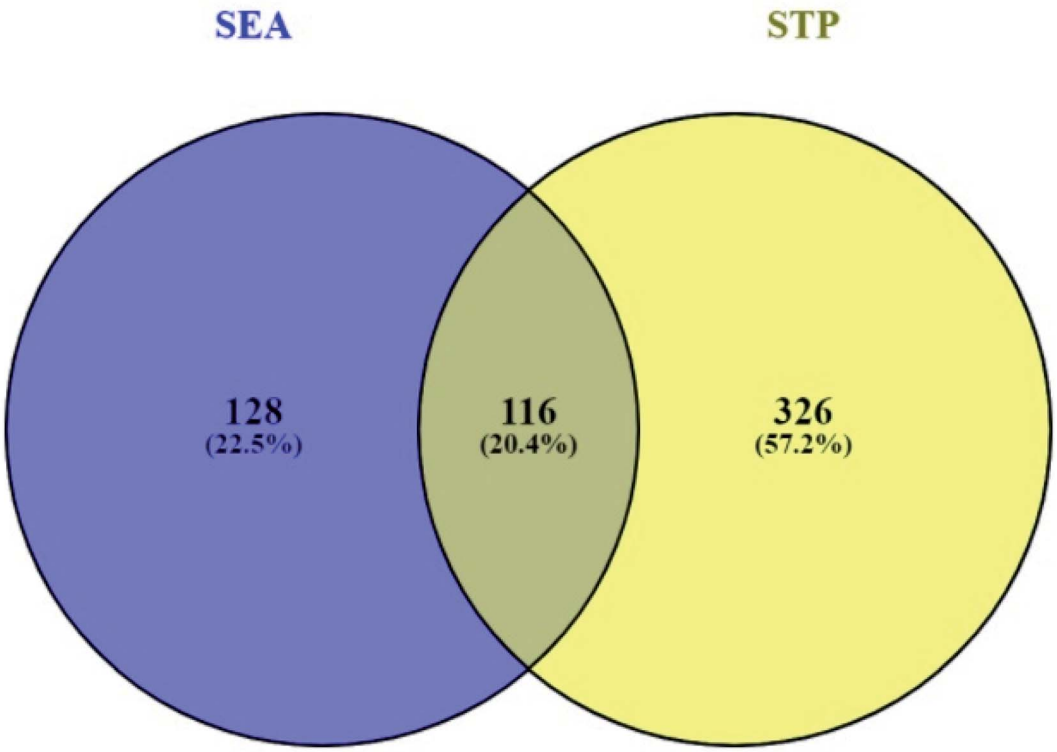

Fig. 3 Overlapping genes (116 genes) between SEA (244 genes) and STP (442 genes).

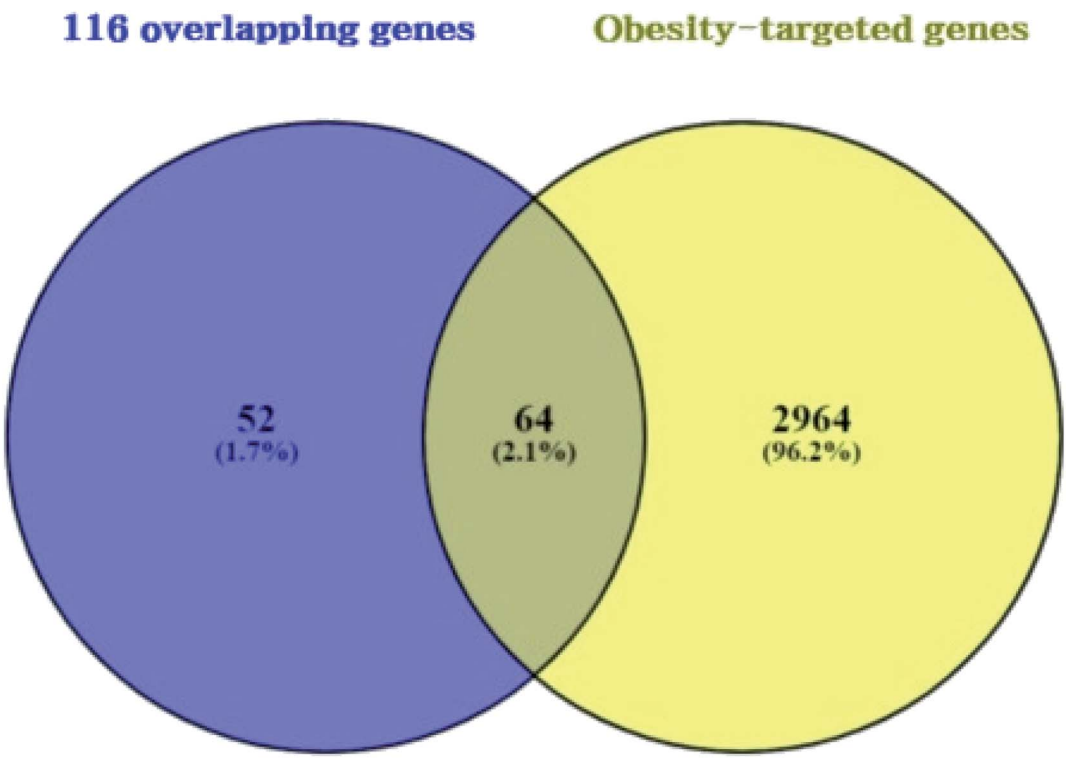

Fig. 4 Overlapping genes between 116 overlapping genes (figure as mentioned earlier 3) from two databases (A) and obesity targeted genes (3028 genes).

diagram's result unveiled 64 overlapping genes that were identified between 3028 genes related to obesity and the 116 overlapping genes (Fig. 4) (ESI Table S3†). As shown in ESI Table S4.† A total of 64 overlapping genes linked to 22 compounds from the 30 compounds mentioned above were identified, retrieving from both SEA and STP public databases, and no genes were found associated with the other 8 compounds (1-methoxycyclohexa-1,3-diene; 2,4-diamino-6-pyrimidinone; 3,4-pentadienal; 3-hydroxy-2,3-dihydromaltol; 5-(hydroxymethyl) furfural; 2-thio-6-azauracil; 2-furanone; 2,3-dihydro-5*H*-1,4-dioxepine) in the two databases.

3.4 Protein–protein network analysis of 22 compounds of HCLLs against obesity

From STRING analysis, 59 out of 64 overlapping genes were closely associated, indicating 59 nodes and 163 edges (Fig. 5). The other (removed) 5 genes (ERN1, SLC22A6, PAM, ADH1B, and GSTK) had no association with the overlapping 64 genes. In the protein–protein interaction (PPI), the AKT1 gene with the highest degree (24) was considered as a hub gene (Table 3).

3.5 Pathway(s)–target protein(s)–compound(s) network analysis of HCLLs against obesity

Pathway(s)–target protein(s)–compound(s) of HCLLs are exhibited in Fig. 6. There were 19 bioactives, 22 target proteins, and 13 pathways (54 nodes, 200 edges). The nodes represented a total number of bioactives, target proteins, and pathways. The edges represented relationships of the three components. The pathway(s)–target protein(s)–compound(s) relationship suggested that the network might interact with therapeutic efficacy against obesity.

3.6 Finding of a hub signaling and hub gene of HCLLs against obesity

The result of KEGG (Kyoto Encyclopedia of Genes and Genomes) pathway enrichment analysis demonstrated that 64

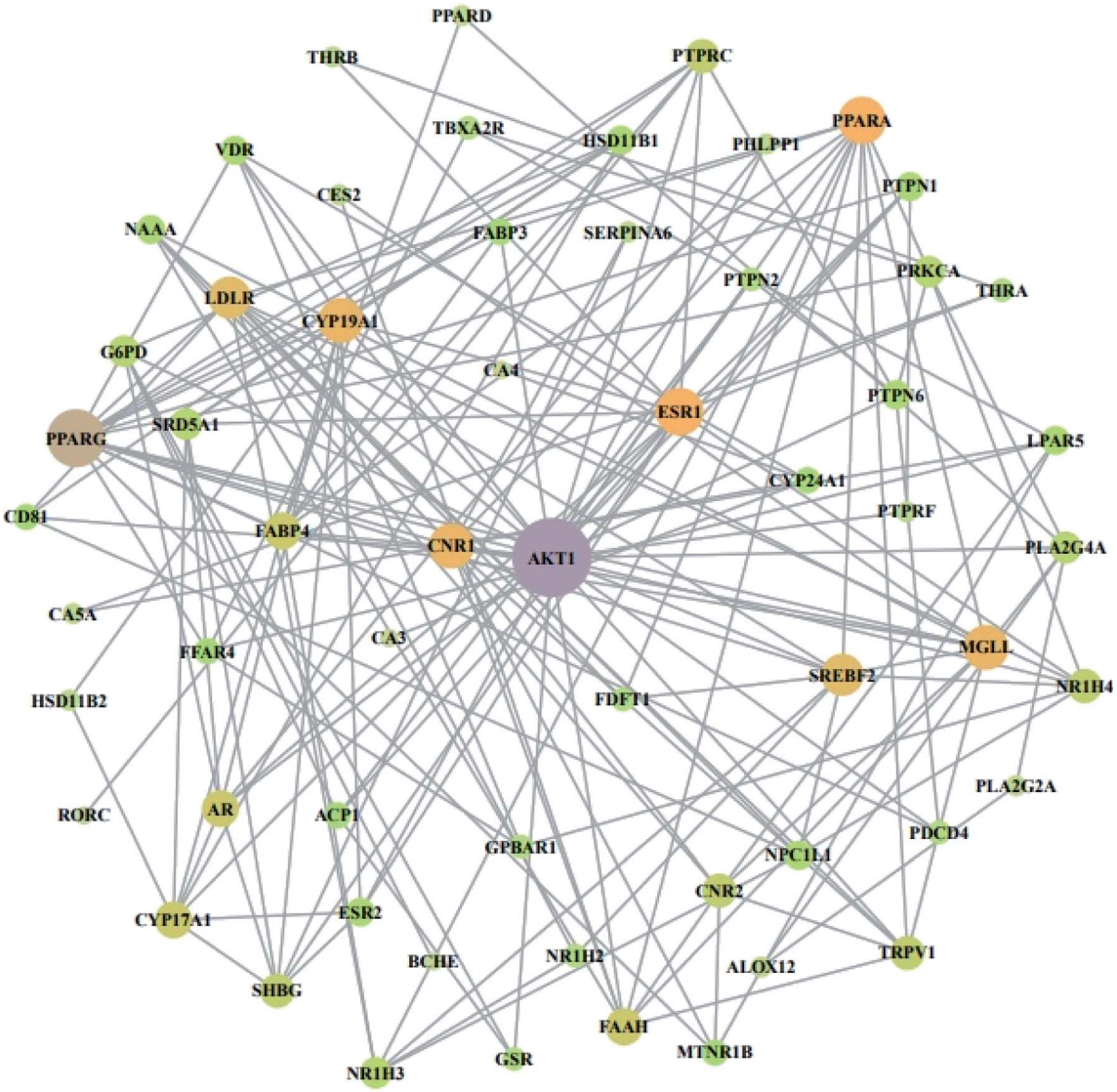

Fig. 5 PPI network against obesity. Nodes: the number of networks of compounds; edges: interactions between compounds and genes.

Table 3 Degree of values of target proteins

No.	Gene symbol	Degree	No.	Gene symbol	Degree
1	AKT1	24	31	NAAA	5
2	PPARG	16	32	ACP1	4
3	ESR1	12	33	CD81	4
4	PPARA	12	34	CYP24A1	4
5	CNR1	11	35	FABP3	4
6	CYP19A1	11	36	FFAR4	4
7	MGLL	11	37	MTNR1B	4
8	LDLR	10	38	FDFT1	3
9	SREBF2	10	39	GPBAR1	3
10	AR	8	40	NR1H2	3
11	CYP17A1	8	41	PDCD4	3
12	FAAH	8	42	PTPN2	3
13	FABP4	8	43	THRA	3
14	CNR2	7	44	GSR	3
15	TRPV1	7	45	TBXA2R	3
16	NR1H4	7	46	ALOX12	2
17	PTPRC	7	47	CA5A	2
18	SHBG	7	48	CES2	2
19	G6PD	6	49	PLA2G2A	2
20	NR1H3	6	50	SERPINA6	2
21	PLA2G4A	6	51	PHLPP1	2
22	PRKCA	6	52	PTPRF	2
23	SRD5A1	6	53	HSD11B2	2
24	ESR2	5	54	THRB	2
25	HSD11B1	5	55	PPARD	2
26	LPAR5	5	56	BCHE	1
27	NPC1L1	5	57	CA3	1
28	PTPN1	5	58	CA4	1
29	PTPN6	5	59	RORC	1
30	VDR	5			

genes were related to 13 signaling pathways (false discovery rate < 0.05). The 13 signaling pathways were directly associated with obesity and indicated that these 13 signaling pathways might be the significant pathways of HCLLs against obesity. The description of 13 signaling pathways is shown in Table 4. Additionally, a bubble chart suggested that the RAS signaling pathway might be a hub signaling pathway of HCLLs against T2DM (Fig. 7). Among 13 signaling pathways, the AKT1 gene was associated with 11 signaling pathways, representing the highest degree of value (Fig. 8). It suggested that AKT1 might be a1 hub gene of HCLLs against obesity.

3.7 MD of 4 genes and 11 compounds related to the RAS signaling pathway

From the SEA and STP databases, it was revealed that the AKT1 gene was associated with three compounds (vitamin E, octyl adipate, and monopalmitin), the PRKCA gene with eight compounds (octyl adipate, monopalmitin, methyl elaidolinolenate, oleic acid, stearic acid, palmitic acid, phytol, and loliolid), the PLA2G2A gene with six compounds (octyl adipate, oleic acid, stearic acid, palmitic acid, 1-methyl-3-piperidinol, and loliolid), and the PLA2G4A gene with three compounds (oleic acid, stearic acid, and palmitic acid).

The MD was performed to evaluate the ligand–protein affinity of these four genes against their association with each gene and the highest ligand–protein docking figures are depicted in Fig. 9. AKT1 protein (PDB ID: 1UNQ) connected to the three compounds on the RAS signaling pathway was subjected to MD. It was observed that vitamin E (-5.5 kcal mol^{-1}) docked on AKT1 protein (PDB ID: 1UNQ) had the greatest binding energy, followed by monopalmitin (-5.3 kcal mol^{-1}) and octyl adipate (-4.8 kcal mol^{-1}). The MD score of eight compounds on PRKCA protein (PDB ID: 3IW4) was analyzed in the "*Homo Sapiens*" setting. It was exposed that monopalmitin (-6.7 kcal mol^{-1}) docked on PRKCA protein (PDB ID: 3IW4) had the highest binding energy, followed by octyl adipate (-6.2 kcal mol^{-1}), loliolid (-5.8 kcal mol^{-1}), phytol (-5.6 kcal mol^{-1}), methyl elaidolinolenate (-5.3 kcal mol^{-1}), oleic acid (-4.9 kcal mol^{-1}), palmitic acid (-4.7 kcal mol^{-1}), and stearic acid (-4.2 kcal mol^{-1}). The MD score of six compounds on PLA2G2A protein (PDB ID: 1KVO) was analyzed in the "*Homo Sapiens*" setting. It was revealed that octyl adipate (-6.2 kcal mol^{-1}) docked on PLA2G2A protein (PDB ID: 1KVO) had the highest binding energy, followed by stearic acid (-6.0 kcal mol^{-1}), loliolid (-5.8 kcal mol^{-1}), oleic acid (-5.2 kcal mol^{-1}), palmitic acid (-5.2 kcal mol^{-1}), and 1-methyl-3-piperidinol (-4.3 kcal mol^{-1}). The MD score of the three compounds on PLA2G4A protein (PDB ID: 1BCI) was analyzed in the "*Homo Sapiens*" setting. It was observed that stearic acid (-4.4 kcal mol^{-1}) docked on PLA2G4A protein (PDB ID: 1BCI) had the highest binding energy, followed by oleic acid (-3.4 kcal mol^{-1}) and palmitic acid (-3.1 kcal mol^{-1}). Collectively, these results showed that the affinity of each compound was not striking a binding score. The docking results are shown in Table 5. It implies that 11 compounds connected to the RAS signaling pathway (a hub signaling pathway) might have a low potency level on target proteins (AKT1, PRKCA, PLA2G2A, PLA2G4A).

3.8 Finding auxiliary signaling over a hub-signaling pathway against obesity

Based on the RichFactor value on each signalling pathway's bubble chart, another distinguished signaling pathway was the PPAR signaling pathway with the highest RichFactor. Noticeably, the AKT1 gene was not associated with the PPAR signaling pathway on the lowest false discovery rate (3.33×10^{-7}). It implies that the PPAR signaling pathway not related to a hub gene might function as auxiliary signaling.

3.9 MD of 6 genes and 14 compounds related to the PPAR signaling pathway

From SEA and STP databases, it was observed that the NR1H3 gene was connected to six compounds (clionasterol, methyl elaidolinolenate, α-amyrin, linolenyl alcohol, 9,12,15-octadecatrienol, and oleic acid), the PPARA gene was related to eleven compounds (oleic acid, palmitic acid, stearic acid, squalene, linolenyl alcohol, 9,12,15-octadecatrienol, methyl elaidolinolenate, citronellylacetone, α-amyrin, clionasterol, and cyclopentaneundecanoic acid, methyl ester), the PPARD gene was associated with ten compounds (oleic acid, palmitic acid, stearic acid, linolenyl alcohol, 9,12,15-octadecatrienol, methyl

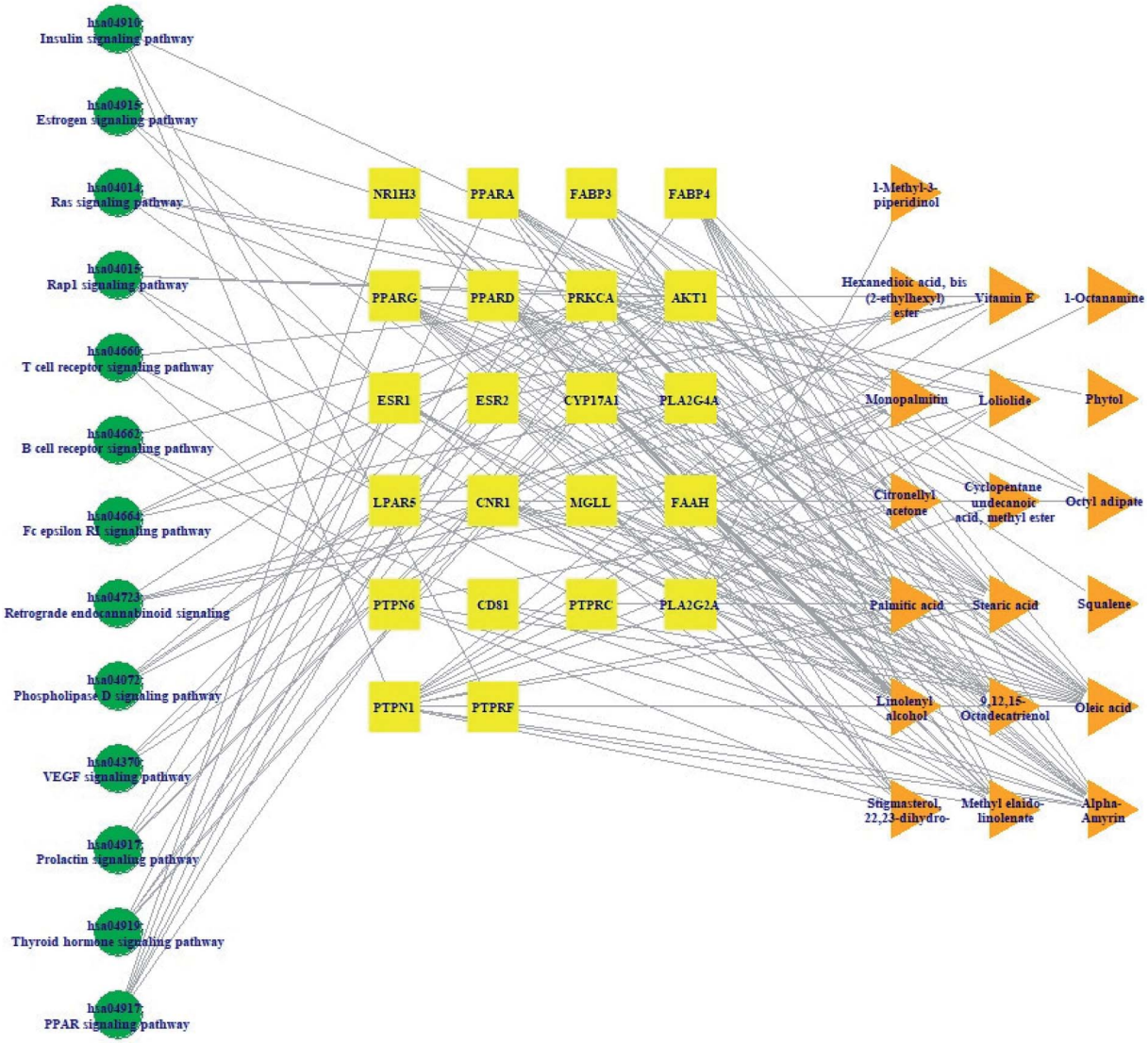

Fig. 6 Pathway(s)–target protein(s)–compound(s) network.

Table 4 Target genes in 13 signaling pathways enrichment related to obesity

KEGG ID & description	Target genes	False discovery rate
has03320: PPAR signaling pathway	NR1H3, PPARA, FABP3, FABP4, PPARG, PPARD	0.0000333
hsa04919: thyroid hormone signaling pathway	PRKCA, AKT1, ESR1, THRA, THRB	0.0012
hsa04917: prolactin signaling pathway	AKT1, ESR1, ESR2, CYP17A1	0.0019
hsa04370: VEGF signaling pathway	AKT1, PRKCA, PLA2G4A	0.012
hsa04072: phospholipase D signaling pathway	AKT1, PRKCA, PLA2G4A, LPAR5	0.0138
hsa04723: retrograde endocannabinoid signaling	PRKCA, CNR1, MGLL, FAAH	0.014
hsa04664: Fc epsilon RI signaling pathway	AKT1, PRKCA, PLA2G4A	0.014
hsa04662: B cell receptor signaling pathway	AKT1, PTPN6, CD81	0.0143
hsa04660: T cell receptor signaling pathway	AKT1, PTPRC, PTPN6	0.0259
hsa04015: Rap1 signaling pathway	AKT1, PRKCA, CNR1, LPAR5	0.0259
hsa04014: ras signaling pathway	AKT1, PRKCA, PLA2G4A, PLA2G2A	0.0347
hsa04915: estrogen signaling pathway	AKT1, ESR1, ESR2	0.0433
hsa04910: insulin signaling pathway	AKT1, PTPN1, PTPRF	0.0433

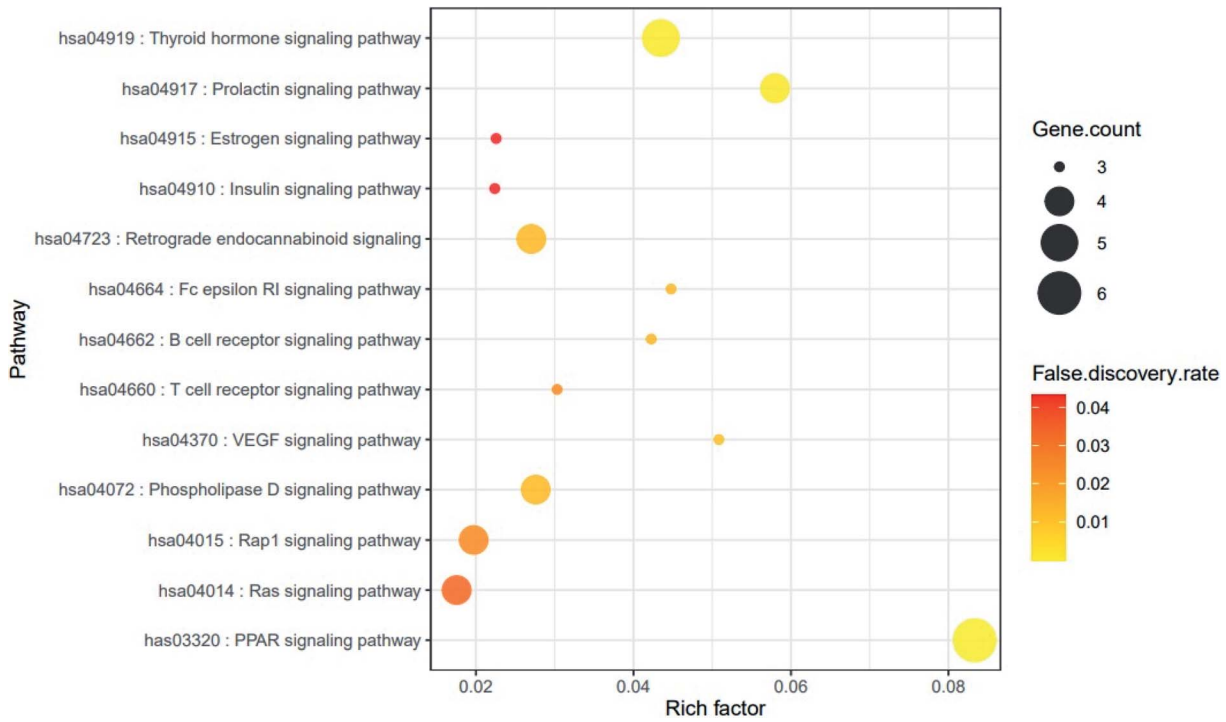

Fig. 7 Bubble chart of 13 signaling pathways connected to the occurrence and development of obesity.

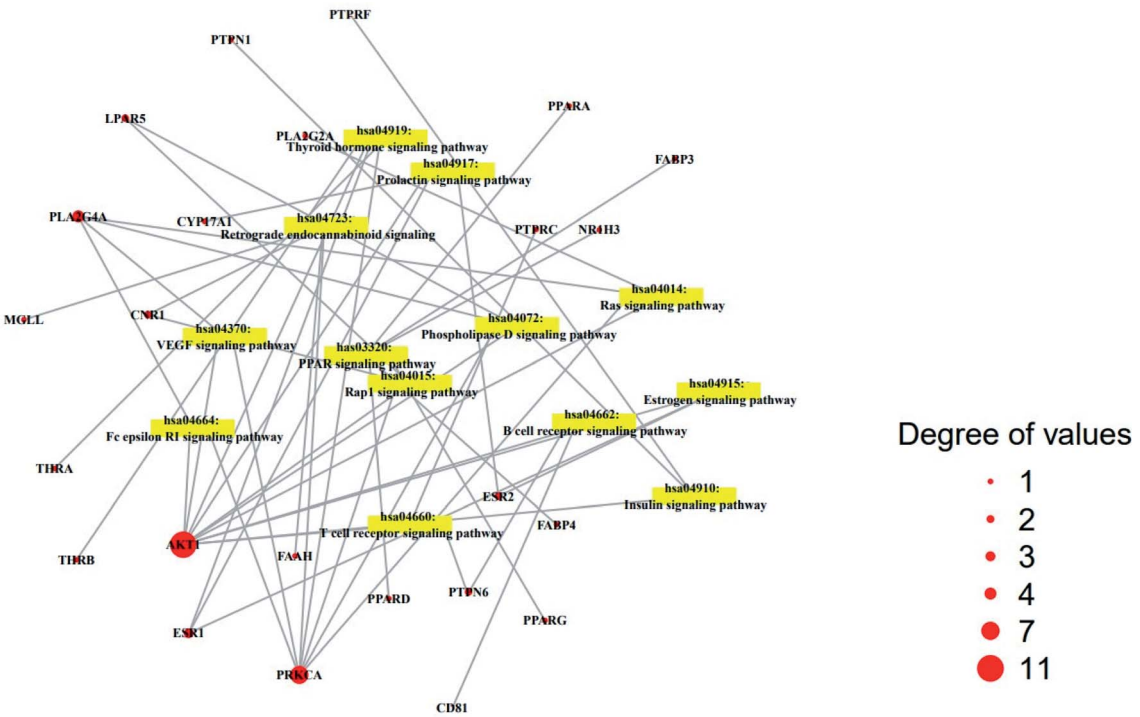

Fig. 8 Degree values of 22 compounds connected to 13 signaling pathways.

elaidolinolenate, citronellylacetone, clionasterol, α-amyrin, and cyclopentaneundecanoic acid, methyl ester), the PPARG gene was involved with ten compounds (oleic acid, palmitic acid, stearic acid, methyl elaidolinolenate, loliolide, linolenyl alcohol, 9,12,15-octadecatrienol, citronellylacetone, α-amyrin, and clionasterol), the FABP3 gene was linked to eleven

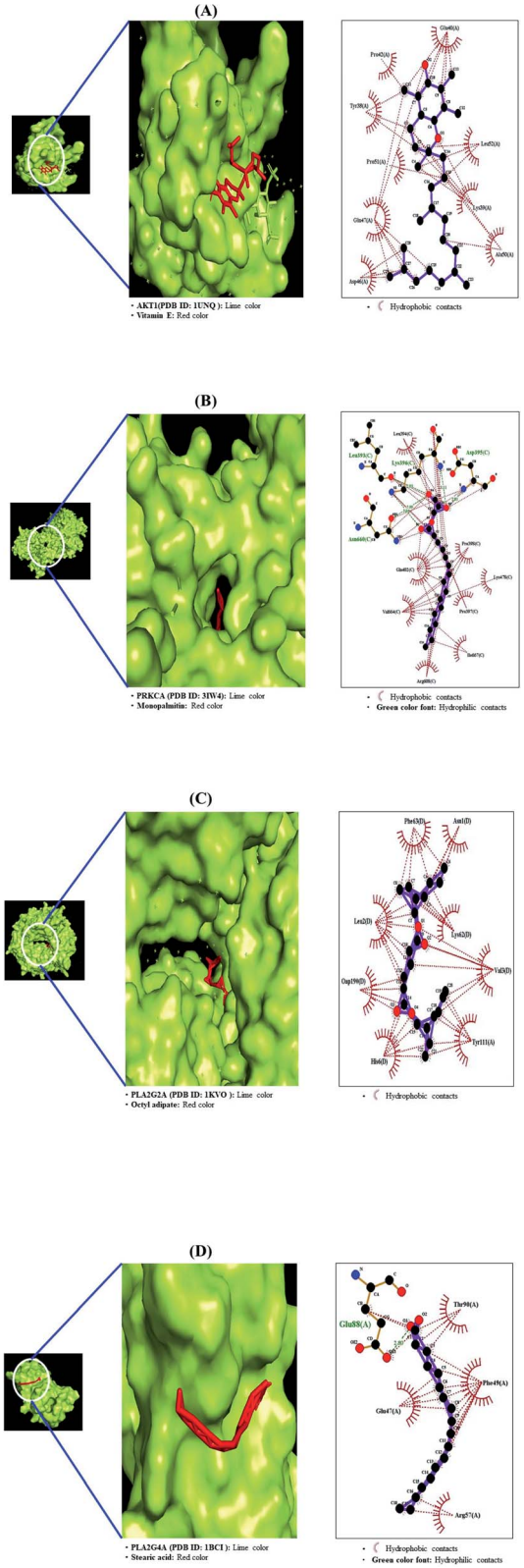

Fig. 9 Molecular docking interaction on RAS signaling pathway between best-docked compounds from HCLLs and target proteins. (A) Vitamin E on AKT1 (PDB ID: 1UNQ) (B) monopalmitin on PRKCA (PDB ID: 3IW4) (C) 1-methyl-3-piperidinol on PLA2G2A (PDB ID: 1KVO) (D) stearic acid on PLA2G4A (PDB ID: 1BCI).

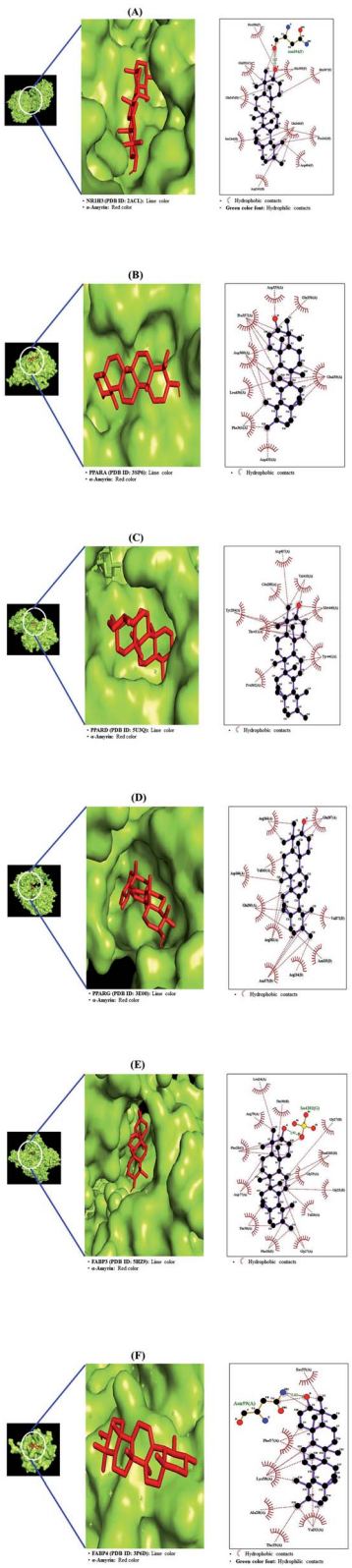

Fig. 10 Molecular docking interaction on PPAR signaling pathway between best-docked compounds from HCLLs and target proteins. (A) α-Amyrin on NR1H3 (PDB ID: 2ACL) (B) α-amyrin on PPARA (PDB ID: 3SP6) (C) α-amyrin on PPARB (PDB ID: 5U3Q) (D) α-amyrin on PPARG (PDB ID: 3E00) (E) α-amyrin on FABP3 (PDB ID: 5HZ9) (F) α-amyrin on FABP4 (PDB ID: 3P6D).

Table 5 Binding energy and interactions of potential active compounds on RAS signaling pathway

Protein	Ligand	PubChem ID	Binding energy (kcal mol^{-1})	Hydrogen bond interactions	Hydrophobic interactions
				Amino acid residue	Amino acid residue
AKT1 (PDB ID: 1UNQ)	Vitamin E	14985	−5.5	N/A	Glu40, Leu52, Lys39 Ala50, Asp46, Gln47 Pro51, Tyr38, Pro42
	Monopalmitin	14900	−5.3	Glu95, Glu91	Val90, Leu12, Trp11 Glu40, Lys39, Pro24 His13
	Octyl adipate	7641	−4.8	Leu52, Lys39	Ala50, Glu40, Pro42 Tyr38, Gln47
PRKCA (PDB ID: 3IW4)	Monopalmitin	14900	−6.7	Leu393, Lys396, Asp395 Asn660	Leu394, Pro398, Lys478 Pro397, Ile667, Arg608 Val664, Gln402
	Octyl adipate	7641	−6.2	N/A	Pro397, Pro398, Gln402 Asn660, Lys396, Leu394 Gln662, Asp395, Glu552 Val664
	Loliolid	100332	−5.8	Arg608, His476, Asp472 Glu552	Glu474, Glu609, Gln548 Asn607, Met551, Ile667
	Phytol	5366244	−5.6	Asp395, Leu393, Lys396	Asn660, Glu552, Gln662 His553, Ser549, Gln548 Val664, Gln402, Pro398 Pro397
	Methyl elaidolinoleate	5367462	−5.3	Lys396, Asn660	Gln402, Val664, Pro397 Pro398, Glu552, Gln662 His553, Glu545, Ser549 Asp539, Leu393, Asp395
	Oleic acid	445639	−4.9	Asp395, Asn660	Gln402, Leu394, Lys396 Gln662, Glu552, Pro398 Pro397, Val664
	Palmitic acid	985	−4.7	Asn660, Lys396, Leu393	Leu394, Gln662, Asp395 Gln402, Pro398, Glu552 Val664, Gln548
	Stearic acid	5281	−4.2	Asn660, Leu393, Lys396	Gln402, Arg608, Pro398 Glu418, Lys478, Pro666 His665, Val664
PLA2G2A (PDB ID: 1KVO)	Octyl adipate	7641	−6.2	N/A	Phe63, Asn1, Lys62 Val3, Tyr111, His6 Leu2
	Stearic acid	5281	−6.0	Val30	Cys28, Phe23, Gly29 Tyr111, Val3, Tyr112 Asn114
	Loliolid	100332	−5.8	Lys115	Thr121, Gly32, Arg33 Lys52, Asp48, Cys49
	Oleic acid	445639	−5.2	Val3	Phe63, Lys62, Phe23 Tyr111, His6, Leu2 Asn1
	Palmitic acid	985	−4.2	Tyr112, Gly25, Asn114, Phe23	Tyr111, His6, Val3 Leu2, Ser113
	1-Methyl-3-piperidinol	98016	−4.3	Cys28, Phe23, Gly25 Tyr112, Asn114	Val30
PLA2G4A (PDB ID: 1BCI)	Stearic acid	5281	−4.4	Glu88	Thr90, Phe49, Arg57 Glu47
	Oleic acid	445639	−3.4	Ile78	Glu76, Phe77, Pro54 Thr53, Leu79, Tyr16
	Palmitic acid	985	−3.1	Ala94	Asn64, Asn95, Arg61 His62, Phe63, Asp43

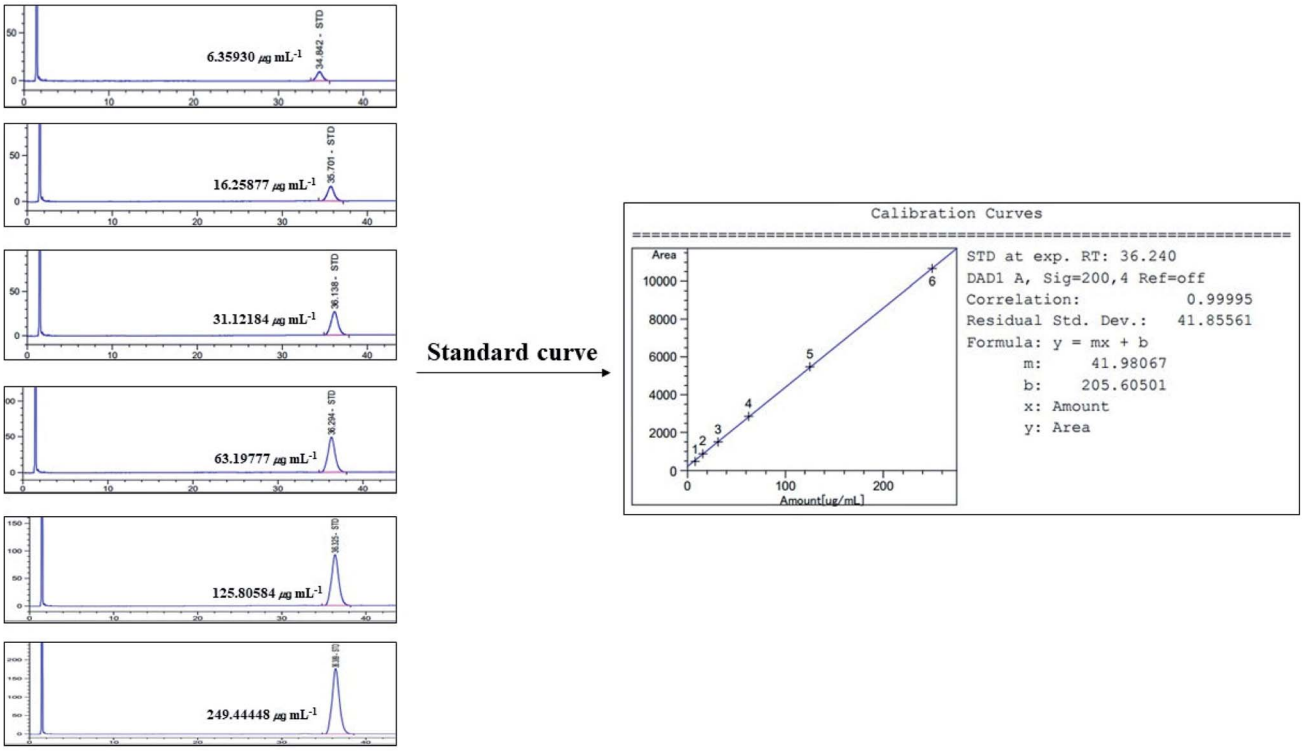

Fig. 11 Standard curve for HPLC/UV analysis of α-amyrin (200 nm).

compounds (oleic acid, linolenyl alcohol, 9,12,15-octadecatrienol, methyl elaidolinolenate, octyl adipate, monopalmitin, palmitic acid, stearic acid, cyclopentaneundecanoic acid, methyl ester, citronellylacetone, and α-amyrin), and the FABP4 gene was connected to nine compounds (oleic acid, palmitic acid, stearic acid, methyl elaidolinolenate, linolenyl alcohol, 9,12,15-octadecatrienol, cyclopentaneundecanoic acid, methyl ester, citronellylacetone, and α-amyrin). In addition, the STRING analysis exhibited an inter-correlation between six genes (PPI enrichment *p*-value: 2.96×10^{-9}) (Fig. 10). MD was performed to evaluate the ligand-protein affinity of these six genes against their associated ones with each gene, respectively, and the highest ligand–protein docking affinity figures are depicted in Fig. 11. The MD score of six compounds on NR1H3 protein (PDB ID: 2ACL) was analyzed in the "*Homo Sapiens*" setting. It was revealed that α-amyrin (-9.7 kcal mol^{-1}) docked on NR1H3 protein (PDB ID: 2ACL) showed the highest binding energy, followed by clionasterol (-8.1 kcal mol^{-1}), methyl elaidolinolenate (-5.3 kcal mol^{-1}), oleic acid (-4.9 kcal mol^{-1}), 9,12,15-octadecatrienol (-4.8 kcal mol^{-1}) and linolenyl alcohol (-4.8 kcal mol^{-1}). It was observed that α-amyrin (-7.4 kcal mol^{-1}) docked on PPARA protein (PDB ID: 3SP6) manifested the highest binding energy, followed by clionasterol (-6.7 kcal mol^{-1}), squalene (-6.0 kcal mol^{-1}), stearic acid (-5.7 kcal mol^{-1}), oleic acid (-5.3 kcal mol^{-1}), cyclopentaneundecanoic acid methyl ester (-5.2 kcal mol^{-1}), methyl elaidolinolenate (-4.7 kcal mol^{-1}), palmitic acid (-4.5 kcal mol^{-1}), citronellylacetone (-4.4 kcal mol^{-1}), 9,12,15-octadecatrienol (-4.4 kcal mol^{-1}), and linolenyl alcohol (-3.6 kcal mol^{-1}). It was found that α-amyrin (-8.5 kcal mol^{-1}) docked on PPARD protein (PDB ID: 5U3Q) exhibited the highest binding energy, followed by clionasterol (-6.8 kcal mol^{-1}), stearic acid (-5.7 kcal mol^{-1}), 9,12,15-octadecatrienol (-5.2 kcal mol^{-1}), palmitic acid (-5.0 kcal mol^{-1}), oleic acid (-4.9 kcal mol^{-1}), citronellylacetone (-4.8 kcal mol^{-1}), methyl elaidolinolenate (-4.7 kcal mol^{-1}), cyclopentaneundecanoic acid methyl ester (-4.7 kcal mol^{-1}), and linolenyl alcohol (-4.6 kcal mol^{-1}). It was revealed that α-amyrin (-8.4 kcal mol^{-1}) docked on PPARG protein (PDB ID: 3E00) showed the highest binding energy, followed by clionasterol (-7.3 kcal mol^{-1}), loliolide (-7.1 kcal mol^{-1}), stearic acid (-5.6 kcal mol^{-1}), citronellylacetone (-5.0 kcal mol^{-1}), oleic acid (-4.9 kcal mol^{-1}), 9,12,15-octadecatrienol (-4.8 kcal mol^{-1}), linolenyl alcohol (-4.7 kcal mol^{-1}), palmitic acid (-4.6 kcal mol^{-1}), and methyl elaidolinolenate (-4.3 kcal mol^{-1}). It was observed that α-amyrin (-10.0 kcal mol^{-1}) docked on FABP3 protein (PDB ID: 5HZ9) had the highest binding energy, followed by stearic acid (-9.0 kcal mol^{-1}), monopalmitin (-8.6 kcal mol^{-1}), octyl adipate (-8.5 kcal mol^{-1}), 9,12,15-octadecatrienol (-7.6 kcal mol^{-1}), cyclopentaneundecanoic acid methyl ester (-7.4 kcal mol^{-1}), citronellylacetone (-7.2 kcal mol^{-1}), oleic acid (-7.1 kcal mol^{-1}), methyl elaidolinolenate (-7.0 kcal mol^{-1}), and palmitic acid (-6.9 kcal mol^{-1}). Finally, it was also exposed that α-amyrin (-8.5 kcal mol^{-1}) docked on FABP4 protein (PDB ID: 3P6D) demonstrated the highest binding energy, followed by stearic acid (-6.5 kcal mol^{-1}), methyl elaidolinolenate (-5.3 kcal mol^{-1}),

Table 6 Binding energy and interactions of potential active compounds on PPAR signaling pathway

Protein	Ligand	PubChem ID	Binding energy (kcal mol^{-1})	Hydrogen bond interactions	Hydrophobic interactions
				amino acid residue	Amino acid residue
NR1H3 (PDB ID: 2ACL)	α-Amyrin	73170	−9.7	Asn394	His395, His397, Glu346 Pro242, Arg404, Asp241 Ser244, Gln243, Glu291
	Clionasterol	457801	−8.1	Asn385	Arg251, Trp236, Lys326 Ile238, Glu394, Pro240 Ala391, Leu400, Ala398 Asp229, Lys395, Glu322 Glu388, Pro237
	Methyl elaidolinoleate	5367462	−5.3	Lys408	Glu390, Arg404, Phe340 Pro336, Glu339, Ala343 Asp379, Pro386
	Oleic acid	445639	−4.9	N/A	Glu390, Lys408, Arg342 Glu339, Pro386, Pro240 Glu346, Tyr397, Met407 Arg404
	9,12,15-Octadecatrienol	5367327	−4.8	Glu339	Ala343, Asp379, Glu390 Lys408, Glu346, Ala387 Pro240, Pro386, Arg342
	Linolenyl alcohol	6436081	−4.8	N/A	Arg248, Leu294, Gln429 Ile299, Val331, Leu329 Ala325, Gln33, Arg302 Asp295, Val298, Lys431
PPARA (PDB ID: 3SP6)	α-Amyrin	73170	−7.4	N/A	Asp353, Glu356, Glu439 Asp432, Phe361, Leu436 Asp360, Pro357
	Clionasterol	457801	−6.7	Lys345	Asp360, Pro357, Glu439 His440, Leu443, Asp353 Glu356
	Squalene	638072	−6.0	N/A	Tyr334, Asn336, Ala333 Thr279, Leu254, Il2901 Val332, Ile241, Glu251 Ala250, Cys275, Cys278 Val255
	Stearic acid	5281	−5.7	N/A	Phe361, Asp432, Leu436 Glu439, His440, Leu443 Asp353, Gln442, Ile446 Pro357, Lys358
	Oleic acid	445639	−5.3	N/A	Leu254, Val255, Il2901 Ala250, Ala333, Asn219 Thr283, Met320, Leu321 Val324, Ile317, Thr279 Tyr334, Cys275, Glu251
	Cyclopentaneundecanoic acid methyl ester	535041	−5.2	Ala333	Asn219, Gly335, Leu331 Tyr334, Thr283, Met220 Glu286, Phe218, Met320 Leu321, Ile317, Thr279 Val324, Val332
	Methyl elaidolinoleate	5367462	−4.7	N/A	Asp432, Leu436, Phe361 Asp360, Leu443, Gln442 Glu439, Pro357, Gln435
	Palmitic acid	985	−4.5	N/A	Val255, Lys257, Leu258 Leu254, Ile241, Ala333 Il2901, Cys275, Thr279 Tyr334, Cys278
	Citronellylacetone	102604	−4.4	N/A	Lys364, Asp360, Pro357 Phe361, Glu439, Gln435 Asp432, Leu436
	9,12,15-Octadecatrienol	5367327	−4.4	Thr307, Asn303	Gly390, Leu690, Ser688 Gln691, Val306, Glu462

Table 6 (*Contd.*)

Protein	Ligand	PubChem ID	Binding energy (kcal mol^{-1})	Hydrogen bond interactions: amino acid residue	Hydrophobic interactions: Amino acid residue
					Arg465, Asp466, Lys310 Pro389
	Linolenyl alcohol	6436081	−3.6	Asn393, Asp304	Ile397, Leu391, Leu300 Leu302, Asn303, Val394
PPARB (PDB ID: 5U3Q)	α-Amyrin	73170	−8.5	N/A	Arg407, Val410, Met440 Tyr441, Pro362, Thr411 Tyr284, Glu288
	Clionasterol	457801	−6.8	N/A	Pro268, His181, Lys265 Ser266, Ser271, Glu262 Lys265, Glu262, Ser271
	Stearic acid	5281	−5.7	N/A	Ser271, Glu262, Lys265 Ser266, Pro268, Ser271
	9,12,15-Octadecatrienol	5367327	−5.2	Thr411, Tyr441	Met440, Pro362, Glu288 Tyr284, Arg361
	Palmitic acid	985	−5.0	Thr411, Arg407	Val410, Arg361, Tyr284 Asp360, Pro362, Tyr441 Met440
	Oleic acid	445639	−4.9	N/A	Asp360, Pro362, Tyr284 Val410, Met440, Tyr441 Thr411
	Citronellylacetone	102604	−4.8	Tyr441	Met440, Thr411, Tyr284 Asp360, Pro362
	Methyl elaidolinoleate	5367462	−4.7	N/A	Tyr441, Met440, Thr411 Arg407, Val410, Glu288 Tyr284, Pro362, Arg361
	Cyclopentaneundecanoic acid methyl ester	535041	−4.7	N/A	Pro362, Tyr441, Thr411 Met440, Val410, Arg407 Arg361, Glu288, Tyr284
	Linolenyl alcohol	6436081	−4.6	Tyr441	Arg361, Tyr284, Met440 Glu288, Thr411, Pro362
PPARG (PDB ID: 3E00)	α-Amyrin	73170	−8.4	N/A	Glu207, Val372, Asn335 Arg234, Asn375, Arg202 Glu203, Asp166, Val163 Arg164
	Clionasterol	457801	−7.3	Asn375	Asp166, Val372, Val163 Arg164, Lys165, Glu208 Glu207, Arg202, Glu203 Lys336, Asn335, Ala371
	Loliolide	100332	−7.1	Arg202, Glu351	Thr162, Leu167, Asp337 Lys336, Gln193, Tyr189 Thr168, Tyr169, Tyr192
	Stearic acid	5281	−5.6	N/A	Val163, Arg164, Val205 Glu203, Arg202, Lys336 Val372, Ala376, Asn375 Asp166, Glu208, Glu207 Gln206
	Citronellylacetone	102604	−5.0	N/A	Lys354, Lys336, Arg350 Leu167, Tyr192, Gln193 Tyr169, Tyr189, Asp337 Thr168
	Oleic acid	445639	−4.9	Lys354, Glu351	Thr168, Lys336, Arg202 Tyr192, Leu167, Tyr169 Asp337, Arg350, Gln193
	9,12,15-Octadecatrienol	5367327	−4.8	Asp337	Tyr192, Tyr169, Tyr189 Thr168, Glu351, Glu369 Val372, Lys336, Arg350 Leu167, Gln193
	Linolenyl alcohol	6436081	−4.7	Glu448	Ser380, Lys381, Pro366 Asp441, Phe370, Glu369

Table 6 (*Contd.*)

Protein	Ligand	PubChem ID	Binding energy (kcal mol^{-1})	Hydrogen bond interactions	Hydrophobic interactions
				amino acid residue	Amino acid residue
					Lys373, Gln444, Asp379 Asn377
	Palmitic acid	985	−4.6	N/A	Tyr189, Tyr169, Glu351 Gln193, Lys354, Lys336 Arg350, Thr168, Leu167 Asp337, Tyr192
	Methyl elaidolinoleate	5367462	−4.3	N/A	Lys336, Arg202, Asn335 Glu203, Arg234, Asn375 Glu207, Lys157, Val205 Val372, Glu378, Gln206 Val163
FABP3 (PDB ID: 5HZ9)	α-Amyrin	73170	−10.0	N/A	Leu24, Thr30, Gly27 Gly25, Val26, Phe28 Thr30, Asp77, Phe28 Arg79
	Stearic acid	5281	−9.0	N/A	Phe28, Gln32, Phe58 Val26, Thr122, Asp77 Thr30, Lys59, Val33 Thr57, Lys22, Ala29
	Monopalmitin	14900	−8.6	Phe58, Thr57	Phe28, Gln32, Val33
	Octyl adipate	7641	−8.5	N/A	Phe28, Val33, Gln32 Ala29, Phe58, Met36 Val33, Thr57
	9,12,15-Octadecatrienol	5367327	−7.6	Thr57, Phe58	Gly27, Gly25, Phe28 Gln32, Ala29
	Cyclopentaneundecanoic acid methyl ester	535041	−7.4	N/A	Gly27, Phe28, Phe58 Lys22, Thr57, Gln32
	Citronellylacetone	102604	−7.2	Lys22	Thr57, Gln32, Ala29
	Oleic acid	445639	−7.1	N/A	Gly27, Gly25, Gln32 Ala29, Phe28
	Methyl elaidolinoleate	5367462	−7.0	N/A	Gly25, Gly27, Ala29 Phe58, Lys22, Phe28
	Palmitic acid	985	−6.9	Gly25	Phe28, Gly27, Gln32 Ala29, Val33, Met36 Thr57
FABP4 (PDB ID: 3P6D)	α-Amyrin	73170	−8.5	Asn59	Ser55, Val32, Thr29 Ala28, Lys58, Phe57
	Stearic acid	5281	−6.5	N/A	Ser1, Ile49, Asp47 Leu66, Leu86, Gly88 Met0
	Methyl elaidolinoleate	5367462	−5.3	Gly88	Asp87, Leu86, Ser1 Asp47, Ile65, Leu66 Met0
	Cyclopentaneundecanoic acid methyl ester	535041	−5.0	N/A	Ser1, Met0, Leu86 Leu66, Asp47, Ile49
	Citronellylacetone	102604	−4.5	Lys120	Lys100, Met119, Ser101
	9,12,15-Octadecatrienol	5367327	−4.4	N/A	Leu86, Leu66, Asp47 Ile49, Ser1
	Oleic acid	445639	−4.4	Leu86, Gly88	Asp87, Leu66, Asp47 Ser1
	Linolenyl alcohol	6436081	−4.4	Gly88, Leu86	Asp87, Cys1, Leu66 Ser1, Met0
	Palmitic acid	985	−4.0	Leu86	Thr85, Gly88, Met0 Leu66

cyclopentaneundecanoic acid methyl ester (−5.0 kcal mol^{-1}), citronellylacetone (−4.5 kcal mol^{-1}), 9,12,15-octadecatrienol (−4.4 kcal mol^{-1}), oleic acid (−4.4 kcal mol^{-1}), linolenyl alcohol (−4.4 kcal mol^{-1}), and palmitic acid (−4.0 kcal mol^{-1}). Noticeably, α-amyrin had the greatest docking score on all six proteins. The docking results are displayed in Table 6.

3.10 Comparative investigation of the docking score against positive controls on target proteins

A comparative MD was performed to evaluate the affinity strength of the highest docking score ligand (α-amyrin) – target proteins. Each positive control of the target protein is as follows. The MD score of GW3965 (PubChem ID: 16078973) on NR1H3 protein (PDB ID: 2ACL) was −11.9 kcal mol^{-1}, where α-amyrin had −9.7 kcal mol^{-1}. The GW3965 (PubChem ID: 16078973) showed a stronger binding affinity than α-amyrin. The MD scores of clofibrate (PubChem ID: 2796), gemfibrozil (PubChem ID: 3463), ciprofibrate (PubChem ID: 2763), bezafibrate (PubChem ID: 39042), and fenofibrate (PubChem ID: 3339) on PPARA protein (PDB ID: 3SP6) were −6.4 kcal mol^{-1}, −6.3 kcal mol^{-1}, −5.4 kcal mol^{-1}, −5.8 kcal mol^{-1}, and −5.4 kcal mol^{-1}, respectively. Interestingly, the MD score of α-amyrin on PPARA protein was more substantial (−7.4 kcal mol^{-1}) than that of five standard drugs. The MD score of cardarine (PubChem ID: 9803963) on PPARD (PDB ID: 5U3Q) was −8.5 kcal mol^{-1}, while α-amyrin docking score was the same as cardarine (PubChem ID: 9803963). The MD scores of pioglitazone (PubChem ID: 4829), rosiglitazone (PubChem ID: 77999), and lobeglitazone (PubChem ID: 9826451) on PPARG (PDB ID: 3E00) were −7.7 kcal mol^{-1}, −7.4 kcal mol^{-1}, and −7.3 kcal mol^{-1}, respectively. Noticeably, the MD score of α-amyrin exposed a stronger binding affinity (−8.4 kcal mol^{-1}) than the three standard drugs. The detailed information is enlisted in Table 7.

3.11 Potential bioactive and signaling pathways of HCLLs against obesity

The MD results of α-amyrin on the PPAR signaling pathway revealed a high binding affinity score. In addition, α-amyrin on 4 proteins (NR1H3, PPARA, PPARD, and PPARG) out of 6 proteins on the PPAR signaling pathway indicated a higher docking score than that of the positive controls (standard drugs). The other 2 proteins (FABP3, FABP4) were not the standard drugs to compare with α-amyrin. Coincidently, α-amyrin might play an essential role in PPAR signaling pathways, suggesting that the PPAR signaling pathway might be an auxiliary signaling pathway of HCLLs against obesity, instead of the RAS signaling pathway.

3.12 Linearity of standard α-amyrin

Linearity was evaluated by the standard curve, determined using 6 different concentrations of α-amyrin dissolved in MeOH. The peak area was acquired to calculate the correlation coefficient of square linear regression analysis. The linearity of peak area responses *versus* concentrations was identified in the range of 6.359 μg mL^{-1} to 249.444 μg mL^{-1} ($r = 0.99995$, $n = 6$) (Fig. 11).

3.13 The identification of α-amyrin from HCLLs

The retention time of α-amyrin was 36.294 min during the HPLC analysis, which exactly overlapped with that of the standard solution. The α-amyrin amount was 9.63489 μg mL^{-1} in HCLLs MeOH extraction (20 μg mL^{-1}) (Fig. 12). The amount of α-amyrin was about 0.05% in HCLLs MeOH extract.

3.14 A hub and an auxiliary signaling pathway among 13 signaling pathways

The selection of the optimal organic solvent is crucial to obtain various bioactive compounds from medicinal plants. Several essential metabolites (alkaloids, flavonoids, tannins and terpenoids) and some non-polar natural compounds are highly soluble in methanol. The high polarity index value of methanol stimulates the extraction rate. Hence, methanol is substantially utilized in medicinal plant extraction to prove medicinal plants' potentiality, and we used MeOH for the extraction of HCLLs.[26] Then, we performed GC-MS analysis, PPI network, signaling pathway analysis, and MD was finally performed through HPLC analysis for an uppermost bioactive compound (α-amyrin).

Compound-genes network indicated that the therapeutic effect of HCLLs on obesity was directly associated with 22 compounds, 64 genes, and 13 signaling pathways against obesity. Based on each gene's degree of value in 13 signaling pathways, AKT1 on the RAS signaling pathway was considered a hub gene of HCLLs against obesity. However, each compound's binding affinity (vitamin E, octyl adipate, and monopalmitin) connected to AKT1 on the RAS signaling pathway revealed a low score through MD. It might be to inhibit the RAS signaling pathway. Meanwhile, the PPAR signaling pathway might function as an auxiliary mode over the RAS signaling pathway. The measurement of ligand–protein binding affinity demonstrated that α-amyrin had a stronger affinity than PPAR agonists. A study suggested that mice (fed a high-fat diet) treated with α,β-amyrin exhibited a significant reduction in body weights, visceral fat, levels of blood glucose, plasma lipids, amylase and lipase activation relative to their respective controls (no treatment of α,β-amyrin).[27] Another animal study indicated that mice treated with α,β-amyrin had a significant drop in blood glucose, total cholesterol, and serum triglyceride levels. Hence, the authors concluded that it could be a lead compound for drug development in metabolic disorders.[28] Additionally, it was reported that treatment of α,β-amyrin (6.25–50 μg mL^{-1}) exerted an anti-adipogenic efficacy *via* the control of lipid and carbohydrate metabolism in 3T3-L1 pre-adipocytes.[29] A study suggested that α,β-amyrin showed a pronounced antiobesity effect on high-fat diet mice,[30] suggesting that α,β-amyrin exposed high enough pharmacological relevance.

Compounds-gene network showed that the therapeutic effect of HCLLs on obesity was directly connected to 64 genes. The results of the KEGG pathway enrichment analysis of 64 genes demonstrated that 13 signaling pathways were directly associated with the occurrence and development of obesity, suggesting that these signaling pathways might be the mechanisms of HCLLs against obesity. The relationships of the 13 signaling pathways with obesity are succinctly discussed as follows. The thyroid hormone signaling pathway: the fast

Table 7 Comparative binding energy between positive controls and α-Amyrin on PPAR signaling pathway

		Docking score (kcal mol^{-1})					
Compounds	PubChem ID	NR1H3 (PDB ID: 2ACL)	PPARA (PDB ID: 3SP6)	PPARB (PDB ID: 5U3Q)	PPARG (PDB ID: 3E00)	FABP3 (PDB ID: 5HZ9)	FABP4 (PDB ID: 3P6D)
α-Amyrin	225688	−9.7	—	—	—	—	—
[a]GW3965	16078973	−11.9	—	—	—	—	—
α-Amyrin	225688	—	−7.4	—	—	—	—
[b]Clofibrate	2796	—	−6.4	—	—	—	—
[b]Gemfibrozil	3463	—	−6.3	—	—	—	—
[b]Ciprofibrate	2763	—	−5.4	—	—	—	—
[b]Bezafibrate	39042	—	−5.8	—	—	—	—
[b]Fenofibrate	3339	—	−5.4	—	—	—	—
α-Amyrin	225688	—	—	−8.5	—	—	—
[c]Cardarine	9803963	—	—	−8.5	—	—	—
α-Amyrin	225688	—	—	—	−8.4	—	—
[d]Pioglitazone	4829	—	—	—	−7.7	—	—
[d]Rosiglitazone	77999	—	—	—	−7.4	—	—
[d]Lobeglitazone	9826451	—	—	—	−7.3	—	—

[a] NR1H3 agonist. [b] PPARA agonist. [c] PPARD agonist. [d] PPARG agonist.

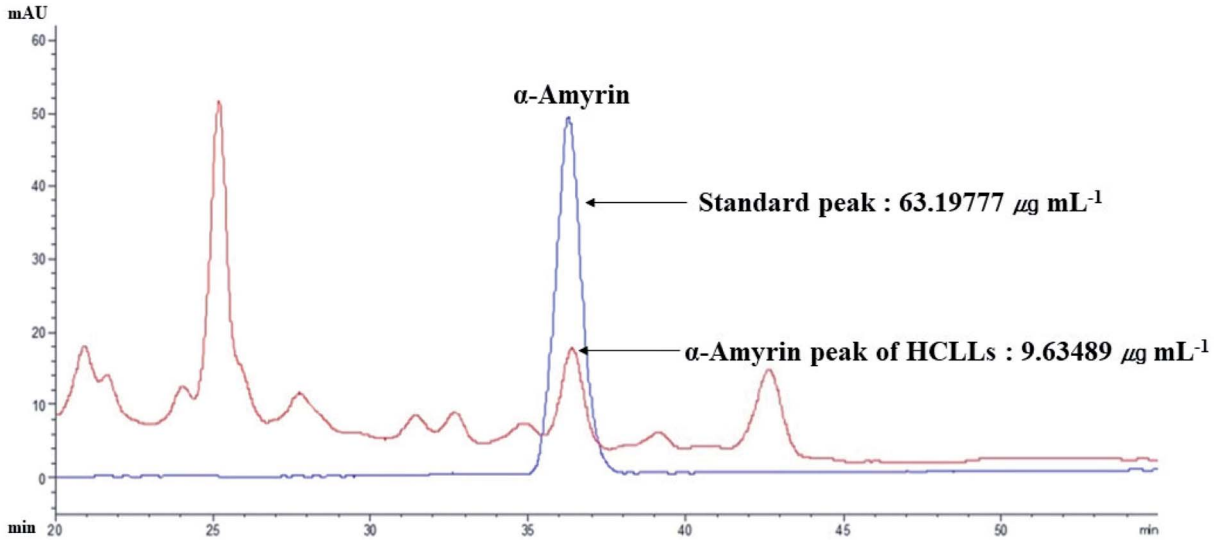

Fig. 12 Overlapping HPLC chromatograms obtained by standard α-amyrin (blue curve) and α-amyrin (red curve) in HCLLs MeOH extraction, wavelength = 200 nm.

weight loss is related to reducing TSH (Thyroid Stimulating Hormone) and T3 (Triiodothyronine). Moreover, due to the Resting Energy Expenditure (REE) decrease, weight loss may be difficult to maintain.[31] Prolactin signaling pathway: prolactin treatment to diet-induced obese rats enhanced the insulin sensitivity that promoted the antiobesity.[32] Estrogen signaling pathway: estrogen receptor α (ER α) mRNA expression levels in non-obese women were lower in obese women in subcutaneous adipose tissue and adipocytes.[33] A study showed that liver ER α–knockout (LKO) male mice had weak insulin sensitivity compared to the wild-type, where estrogens played an important biological role in the modulation of metabolism and obesity.[34] The insulin signaling pathway: in chronic obesity, the expression level of diverse insulin signaling molecules decreased in skeletal muscle that dysregulated the insulin receptor.[35] Retrograde endocannabinoid signaling: cannabinoid type 1 receptor (CB1R) -induced signaling had been exhibited to lead to metabolic inactivation. In contrast, the interruption of the CB1R function could alleviate several obesity-induced causal factors in metabolism.[36] Fc epsilon RI (FcεRI) signaling pathway: FcεRI suppressed body weight gain and enhanced glucose tolerance in diet-induced obese mice. It implies that FcεRI is an efficient mediator to mitigate obesity.[37] B cell receptor signaling pathway: obese individuals have lower antibody production to influenza vaccination than non-obese individuals. Besides, mice experiments

demonstrated that obese mice had lower productivity of haemagglutination inhibition (HAI) antibodies.[38] T cell receptor signaling pathway: T cell dysfunction due to obesity induces proinflammatory cytokines, which correlate with abnormal immunity.[39] VEGF signaling pathway: VEGF release rate from obese subjects of visceral adipose tissue (VAT) was found higher in comparison to subcutaneous adipose tissue (SAT) and VAT of non-obese controls.[40] Phospholipase D signaling pathway: PLD1 (phospholipase D1) or PLD2 (phospholipase D2) deleted mice consumed more food than control groups, specifically, PLD1 and PLD2 repressed appetite and protected against obesity.[41] Rap1 signaling pathway: *Rap1*-lacking mice accumulated fat in the abdomen, hepatic steatosis, and rapid-fasting plasma levels of insulin, glucose, cholesterol, and alanine aminotransferase.[42] RAS signaling pathway: Obesity-associated disorders over-activate RAS, suggesting a significant RAS role in body weight control and enhancing insulin sensitivity.[43] PPAR signaling pathway: PPARs modulate the inflammatory responses, which mitigate obesity-induced inflammation.[44] PPARA or PPARD agonist treatment induced a decrease in fat mass (FM) and PPARB agonist-improved insulin resistance.[45,46] Reports indicated that all the 13 signaling pathways with 22 compounds in HCLLs were connected to the suppression of obesity. Outwardly, the AKT1 gene and vitamin E are related to inactivating the RAS signaling pathway and might be a key mechanism against obesity. However, RAS signaling pathway related compounds and proteins did not result in viable predicted binding energies (>-7.0 kcal mol^{-1}) during MD.

The threshold value of docking binding energy was set up <-7.0 kcal mol^{-1}, which was significantly favorable binding energy.[47] As an alternative approach, 14 compounds and 6 genes associated with the PPAR signaling pathway were selected to generate binding energy. Among 14 compounds, α-amyrin with all 6 proteins (NR1H3, PPARA, PPARD, PPARG, FABP3, and FABP4) showed significant binding energy. From comparative MD, α-amyrin had a higher binding affinity than that of the standard drugs (NR1H3 agonist, PPARA agonists, and PPARG agonists). Only PPARD agonist binding energy was the same as α-amyrin. Although this study identified 14 molecules, α-amyrin exhibited the highest binding affinity mutually in 6 proteins on PPAR signaling pathways. Furthermore, we identified the amount of α-amyrin (9.63489 μg mL^{-1}) from HCLLs (20 mg) MeOH extraction, which was confirmed *via* standard curve validation. Altogether, our study demonstrated the potential effectiveness of the auxiliary signaling pathway of HCLLS in suppressing obesity through network pharmacology analysis.

4. Conclusion

The active molecules and mechanisms of HCLLs against obesity were first confirmed by utilizing network pharmacology. Furthermore, this research suggested that activation of the PPAR signaling pathway is a comparatively promising mechanism than the inactivation of the RAS signaling pathway of HCLLs for antiobesity. A prominent molecule, α-amyrin, might be considered a triple agonist (PPARA, PPARD, PPARG) against obesity. Finally, HPLC analysis identified the amount (0.05%) of α-amyrin in HCLLs, which confirmed the presence of this compound in HCLLs. Therefore, this analysis provides pharmacological evidence to support the efficacy of HCLLs on obesity and expounds an uppermost bioactive compound and mechanism(s) of HCLLs against obesity.

Author contributions

K. K. O.: conceptualization, methodology, formal analysis, investigation, data curation, writing – original draft. K. K. O. and M. A. and I. S. J.: software, investigation, data curation. M. A.: validation, writing – review & editing. D. H. C.: supervision, project administration.

Conflicts of interest

The authors have declared no conflict of interest. They have no known competing financial interests or personal relationships that could have appeared to influence the research reported in this publication.

Abbreviations

BMI	Body mass index
CB1R	Cannabinoid type 1 receptor
GC-MS	Gas chromatography-mass spectrometer
ER-α	Estrogen receptor α
FM	Fat mass
GGQLD	Ge-Gen-Qin-Lian decoction
GSEA	Gene set enrichment analysis
HAI	Haem agglutination inhibition
HCLLs	*Hibiscus cannabinus* L. leaves
KEGG	Kyoto encyclopedia of genes and genomes
LDL-C	Low density lipoprotein – cholesterol
LKO	Liver ER α-knockout
MD	Molecular docking
PDB	Protein data bank
PLD1	Phospholipase D1
PLD2	Phospholipase D2
PPAR	Peroxisome proliferator activated receptor
PPARA	Peroxisome proliferator activated receptor alpha
PPARD	Peroxisome proliferator activated receptor delta
PPARG	Peroxisome proliferator activated receptor gamma
PPI	Protein–protein interaction
RAP1	Repressor activator protein 1
RAS	Renin angiotensin system
REE	Resting energy expenditure
SAT	Subcutaneous adipose tissue
SEA	Similarity ensemble approach
SMILES	Simplified molecular input line entry system
STP	SwissTargetPrediction
TSH	Thyroid stimulating hormone
VEGF	Vascular endothelial growth factor

Acknowledgements

This research was acknowledged by the Department of Bio-Health Convergence, Kangwon National University, Chuncheon 24341, Republic of Korea.

Notes and references

1 K. Bhaskaran, I. Douglas, H. Forbes, I. Dos-Santos-Silva, D. A. Leon and L. Smeeth, *Lancet*, 2014, **384**, 755–765.
2 K. B. Smith and M. S. Smith, *Primary Care: Clinics in Office Practice*, 2016, **43**, 121–135.
3 Obesity and overweight.
4 M. Tremmel, U. G. Gerdtham, P. M. Nilsson and S. Saha, *Int. J. Environ. Res. Public Health*, 2017, **14**, 435.
5 T. T. Liu, X. T. Liu, Q. X. Chen and Y. Shi, *Biomed. Pharmacother.*, 2020, **128**, 110314.
6 Antiobesity Drugs – an overview, ScienceDirect Topics.
7 Y. Liu, M. Sun, H. Yao, Y. Liu and R. Gao, *J. Evidence-Based Complementary Altern. Med.*, 2017, **2017**, 1–17.
8 N. S. Kai, T. A. Nee, E. L. C. Ling, T. C. Ping, L. Kamariah and N. K. Lin, *Asian Pac. J. Trop. Med.*, 2015, **8**, 6–13.
9 J. M. Son, H. S. Ju, H. J. N. Gung, M. O. K. Azad, M. D. Adnan and D. H. Cho, *Korean Journal of Medicinal Crop Science*, 2019, **27**, 89.
10 M. Adnan, M. O. K. Azad, H. S. Ju, J. M. Son, C. H. Park, M. H. Shin, M. Alle and D. H. Cho, *Appl. Nanosci.*, 2019, 1–13.
11 M. C. D. Adnan, M. O. K. Azad, A. Madhusudhan, K. Saravanakumar, X. Hu, M. H. Wang and D. H. Cho, *Nanotechnology*, 2020, **31**, 265101.
12 M. Adnan, K. K. Oh, M. O. K. Azad, M. H. Shin, M.-H. Wang and D. H. Cho, *Life*, 2020, **10**, 223.
13 P. Kumar and U. Bhandari, *Ancient Science of Life*, 2015, **35**, 58.
14 Effect of ethanolic extract of *Hibiscus cannabinus* leaf on high cholesterol diet induced obesity in female albino rats.
15 S. Giwa Ibrahim, R. Karim, N. Saari, W. Z. Wan Abdullah, N. Zawawi, A. F. Ab Razak, N. A. Hamim and R. A. Umar, *J. Food Sci.*, 2019, **84**(8), 2015–2023.
16 R. Zhang, X. Zhu, H. Bai and K. Ning, *Front. Pharmacol.*, 2019, **10**, 1–15.
17 K. K. Oh, M. Adnan and D. H. Cho, *Gene Reports*, 2020, 100851.
18 A. L. Hopkins, *Nat. Chem. Biol.*, 2008, **4**(11), 682–690.
19 K. K. Oh, M. Adnan and D. H. Cho, *PLoS One*, 2020, **15**, e0240873.
20 S. Li and B. Zhang, *Chin. J. Nat. Med.*, 2013, **11**, 110–120.
21 H. Li, L. Zhao, B. Zhang, Y. Jiang, X. Wang, Y. Guo, H. Liu, S. Li and X. Tong, *J. Evidence-Based Complementary Altern. Med.*, 2014, **2014**, 495840.
22 M. J. Keiser, V. Setola, J. J. Irwin, C. Laggner, A. I. Abbas, S. J. Hufeisen, N. H. Jensen, M. B. Kuijer, R. C. Matos, T. B. Tran, R. Whaley, R. A. Glennon, J. Hert, K. L. H. Thomas, D. D. Edwards, B. K. Shoichet and B. L. Roth, *Nature*, 2009, **462**, 175–181.
23 A. Daina, O. Michielin and V. Zoete, *Nucleic Acids Res.*, 2019, **47**, W357–W3664.
24 K. K. Oh, M. Adnan and D. H. Cho, *Gene*, 2020, 145320.
25 P. Khanal, B. M. Patil, J. Chand and Y. Naaz, *Nat. Prod. Bioprospect.*, 2020, **10**, 325–335.
26 M. Adnan, M. N. U. Chy, A. T. M. M. Kamal, J. W. Barlow, M. O. Faruque, X. Yang and S. B. Uddin, *J. Ethnopharmacol.*, 2019, **236**, 401–411.
27 F. Santos, V. Rao, K. Carvalho, T. Morais, A. da Silva and M. Chaves, *Planta Med.*, 2013, **79**, PE14.
28 F. A. Santos, J. T. Frota, B. R. Arruda, T. S. De Melo, A. A. D. C. A. Da Silva, G. A. D. C. Brito, M. H. Chaves and V. S. Rao, *Lipids Health Dis.*, 2012, **11**(98), 1–8.
29 K. M. de Melo, F. T. B. de Oliveira, R. A. Costa Silva, A. L. Gomes Quinderé, J. D. B. Marinho Filho, A. J. Araújo, E. D. Barros Pereira, A. A. Carvalho, M. H. Chaves, V. S. Rao and F. A. Santos, *Biomed. Pharmacother.*, 2019, **109**, 1860–1866.
30 A. Karine Maria Martins Bezerra Carvalho, T. Sousa de Melo, K. Moura de Melo, A. Luiza Gomes Quinderé, F. Tuelly Bandeira de Oliveira, A. Flávia Seraine Custódio Viana, P. Iury Gomes Nunes, J. da Silva Quetz, D. de Araújo Viana, A. André de Carvalho Almeida da Silva, A. Havt, S. Gonçalves da Cruz Fonseca, M. Helena Chaves, V. Satyanarayana Rao and F. Almeida Santos, *Planta Med.*, 2017, **83**, 285–291.
31 T. Reinehr, *Mol. Cell. Endocrinol.*, 2010, **316**, 165–171.
32 X. Ruiz-Herrera, E. A. de los Ríos, J. M. Díaz, R. M. Lerma-Alvarado, L. M. de la Escalera, F. López-Barrera, M. Lemini, E. Arnold, G. M. de la Escalera, C. Clapp and Y. Macotela, *Endocrinology*, 2016, **158**, 1444.
33 M. Nilsson, I. Dahlman, M. Rydén, E. A. Nordström, J. Å. Gustafsson, P. Arner and K. Dahlman-Wright, *Int. J. Obes.*, 2007, **31**, 900–907.
34 L. Zhu, M. N. Martinez, C. H. Emfinger, B. T. Palmisano and J. M. Stafford, *Am. J. Physiol.: Endocrinol. Metab.*, 2014, **306**, E1188.
35 B. B. Kahn and J. S. Flier, *J. Clin. Invest.*, 2000, **106**, 473–481.
36 C. Lipina, W. Rastedt, A. J. Irving and H. S. Hundal, *Wiley Interdiscip. Rev.: Membr. Transp. Signaling*, 2013, **2**, 49–63.
37 Y. J. Lee, C. Liu, M. Liao, G. K. Sukhova, J. Shirakawa, M. Abdennour, K. Iamarene, S. Andre, K. Inouye, K. Clement, R. N. Kulkarni, A. S. Banks, P. Libby and G. P. Shi, *Endocrinology*, 2015, **156**, 4047–4058.
38 S. R. Shaikh, K. M. Haas, M. A. Beck and H. Teague, *Clin. Exp. Immunol.*, 2015, **179**, 90–99.
39 E. G. Aguilar and W. J. Murphy, *Curr. Opin. Immunol.*, 2018, **51**, 181–186.
40 R. Schlich, M. Willems, S. Greulich, F. Ruppe, W. T. Knoefel, D. M. Ouwens, B. Maxhera, A. Lichtenberg, J. Eckel and H. Sell, *Mediators Inflammation*, 2013, **2**, 1–11.
41 J. T. Viera, R. El-Merahbi, B. Nieswandt, D. Stegner and G. Sumara, *PLoS One*, 2016, **11**(6), 1–13.
42 P. Martínez, G. Gómez-López, F. García, E. Mercken, S. Mitchell, J. M. Flores, R. deCabo and M. A. Blasco, *Cell Rep.*, 2013, **3**, 2059–2074.

43 R. Gul, H. Dekhil and A. Alfadda, *Saudi Journal of Obesity*, 2018, **6**, 5.
44 R. Stienstra, C. Duval and S. Kersten, *PPAR Res*, 2007, **2007**, 95974.
45 R. Stienstra, C. Duval, M. Müller and S. Kersten, *PPAR Res.*, 2007, **2007**, 95974.
46 F. M. Silva-Veiga, T. L. Rachid, L. de Oliveira, F. Graus-Nunes, C. A. Mandarim-de-Lacerda and V. Souza-Mello, *Mol. Cell. Endocrinol.*, 2018, **474**, 227–237.
47 R. R. Mohan, M. Wilson, R. D. Gorham, R. E. S. Harrison, V. A. Morikis, C. A. Kieslich, A. A. Orr, A. V. Coley, P. Tamamis, D. Morikis and A. Mcferrin, *ACS Omega*, 2018, **3**, 6427–6438.